ARTICLE

Microfluidic Encapsulation for Controlled Release and its Potential for Nanofertilisers

Received 00th January 20xx,
Accepted 00th January 20xx

DOI: 10.1039/x0xx00000x

Le Nguyen Quang Tu,[a,b] Nam Nghiep Tran,*[a,c], Marc Escribà-Gelonch,[d] Christophe A. Serra,[e] Ian Fisk,[f,g] David Julian McClements[h], Volker Hessel*[a,i]

Nanotechnology is increasingly being utilized to create advanced materials with improved or new functional attributes. Converting fertilizers into a nanoparticle-form has been shown to improve their efficacy but the current procedures used to fabricate nanofertilisers often have poor reproducibility and flexibility. Microfluidic systems, on the other hand, have advantages over traditional nanoparticle fabrication methods in terms of energy and materials consumption, versatility, and controllability. The increased controllability can result in the formation of nanoparticles with precise and complex morphologies (e.g., tuneable sizes, low polydispersity, and multi-core structures). As a result, their functional performance can be tailored to specific applications. This paper reviews the principles, formation, and applications of nano-enabled delivery systems fabricated using microfluidic approaches for the encapsulation, protection, and release of fertilizers. Controlled release can be achieved using two main routes: (i) nutrients adsorbed on nanosupports and (ii) nutrients encapsulated inside nanostructures. We aim to highlight the opportunities for preparing a new generation of highly versatile nanofertilisers using microfluidic systems. We will explore several main characteristics of microfluidically prepared nanofertilisers, including droplet formation, shell fine-tuning, adsorbate fine-tuning, and sustained/triggered release behavior.

1. Introduction

This review is about a novel type of fertiliser, nanofertilisers, and the potential of microfluidic encapsulation to produce them in a new way. The motivation for the development of nanofertilisers is that they can help to prevent soil degradation, reduce pollution, decrease crop losses, and increase crop yields. As a result, their application could enhance global food security. Food security means that there is a sufficient, safe and nutritious food source that is physically, socially and economically accessible to all people at all times and meets their nutrient demands and preferences for an active and healthy life, as stated in the 2009 Declaration of the World Summit on Food Security.[1] In 2014, the Food and Agriculture Organization (FAO) and World Health Organization (WHO) reported that some of the main challenges to food security were associated with resource deficiency, ecosystem degradation, unsustainable production, food losses, and waste and unequal distribution.[2] However, the fundamental role of soil in providing healthy and nutritious food is often overlooked. Soil degradation causes changes in soil functions that eventually affect crop yields. In 2014, over 2 billion people suffered from micronutrient deficiencies which were directly linked to nutrient impoverished soils.[2, 3] This situation is forecast to become worse in 2050 as the population is predicted to exceed 9 billion people and the global demand for food is expected to grow by 60 %, with increases of >100% in developing countries due to their faster income growth.[4, 5] This situation could potentially result in a dilemma in soil management since higher incomes will increase food consumption, followed by higher productivity requirements for agriculture, which will deplete water and soil resources. A growing global population also requires more land for industry and communities, thereby leading to a decrease in usable land for agriculture. Thus, healthy soil is the foundation of sustainable agricultural production, which is critical to provide food security for the world population. Soil threats can be categorized into three major groups: soil degradation, land-use changes, and unsustainable soil management.[6]

Soil degradation has harmful effects on its health by affecting its composition, structure, and functions. Typical forms of degradation include soil erosion, soil contamination, and soil salinization.[6, 7] Soil erosion is defined as the removal of topsoil,

[a] School of Chemical Engineering and Advanced Materials, The University of Adelaide, Adelaide, SA 5005, Australia
[b] Faculty of Chemical Engineering, Ho Chi Minh City University of Technology, Ho Chi Minh City, Vietnam
[c] School of Chemical Engineering, Can Tho University, Can Tho City, Vietnam
[d] Higher Polytechnic Engineering School, University of Lleida, Igualada (Barcelona), 08700, Spain
[e] Université de Strasbourg, CNRS, Institut Charles Sadron UPR 22, F-67000 Strasbourg, France
[f] Division of Food, Nutrition and Dietetics, School of Biosciences, University of Nottingham, Loughborough, LE12 5RD, UK
[g] The University of Adelaide, North Terrace, Adelaide, South Australia, Australia
[h] Department of Food Science, University of Massachusetts, Amherst, MA 01003, USA
[i] School of Engineering, University of Warwick, Library Rd, Coventry, UK
*Author for correspondence. E-mail: volker.hessel@adelaide.edu.au
*Author for correspondence. E-mail: namnghiep.tran@adelaide.edu.au

which contains the organic matter that supplies nutrients and is responsible for the structural stability of soil protection from erosion by wind and water. In general, this reduces the thickness of the topsoil, adversely alters soil properties, and depletes organic matter and nutrients.[8] The impacts may vary across soils and ecoregions, but it is identified that countries with fragile soils, poorly developed markets, harsh climates, and limited access to remediation technologies will suffer the most.[9-11] Soil contamination occurs when an excessive amount of trace metals, agrochemicals, industrial chemicals and urban waste come into contact with land.[12-14] This phenomenon interferes with the breakdown of organic matter and alters the nutrient cycle of soil, which then decreases biodiversity, fertility and soil health dramatically. Furthermore, pollutant build-up in the soil can be absorbed by plants through roots and the prolonged consumption of contaminated food can potentially lead to fatality.[13, 15, 16]

Soil salinization is the result of the accumulation of water-soluble elements, such as sodium, calcium, magnesium, and iron. “Primary salinity” and “secondary salinity” relate to salt accumulation over long periods through natural processes (e.g., seawater intrusion onto land) and mismanagement of natural resources (e.g., overuse of fertilisers), respectively.[17] An excessive amount of salt in soil can obstruct the plant’s ability to uptake water by increasing the osmotic pressure of the soil, reducing crop growth, and resulting in visible changes to the plant. The accumulation of specific ions can also lead to nutritional imbalance and toxicity.[18, 19]

Chemical fertilisers can be used to provide degraded soil with essential nutrients for remediation and help to increase crop productivity. Conventional fertilisers such as urea and nitrogen-phosphate-potassium (NPK) have been used for decades to supply macronutrient elements to plants. Furthermore, specialized fertilisers with micronutrients or elements to change the soil properties have also been used to tackle land degradation. However, the use of conventional fertilisers often causes problems in low nutrient use efficiency and environmental concerns, which are obstacles to enhancing the sustainability of agricultural systems.[20] Less than 50% of the fertilisers applied to the soil are absorbed by the crops. Residual minerals tend to leach out and either accumulate in the soil or contribute to water pollution.[21, 22] Specifically, it has been reported that crops can only absorb 30-60%, 10-20% and 10-50% of N, P and K elements when fertilisers are applied to the soil.[23, 24] Farmers tend to compensate for nutrient loss and achieve higher crop yields by repeating the application of these fertilisers. This leads to a reduction in soil fertility, increases soil salinity, creates a nutritional imbalance in the soil, and causes more severe environmental concerns including water pollution, air pollution, and water eutrophication.[25] Additionally, the over-application of conventional chemical fertilisers increases the cost and reduces the profit margins for farmers. Hence, it is crucial to be able to control the release rate of nutrients in fertilisers to increase crop yield, reduce pollution, and enhance the sustainability of land resources.

Nanotechnology has been used to create advanced materials with new or improved functional properties that are finding increasing use commercially. These materials typically have one or more dimension that falls in the nanoscale region, often taken to be less than 100 nm. However, this definition is sometimes used to cover materials with larger dimensions (< 1000 nm). Reducing the size of materials into the nanoscale alters their functional performance due to the small particle size, high surface-to-volume ratio, and altered surface activity. Moreover, it is often possible to control the structural organization and surface chemistry of materials on the nanoscale, which can lead to desirable functional attributes, such as encapsulation, protection, controlled release, high sorption capacity, and chemical sensitivity.[23] There is therefore great potential for nanotechnology to enhance the performance of conventional fertilizers. For instance, it can be used to create nanofertilisers for the sustained, controlled, or triggered release of essential nutrients to crops precisely when they need them, as well as to reduce the leakage of soluble salts into the environment.[26, 27] For example, the duration over which nutrients (e.g. nitrogen) are released can increase from 4-10 days in the case of conventional chemical fertilisers to 6-7 weeks when using state-of-the-art smart-fertilisers developed using nanotechnology, and the salt does not get accumulated in the soil over time.[28] Table 1 highlights significant studies that compare nano-enabled fertilisers and their conventional equivalents. In this article, we used the term smart-fertilizers to refer to fertilizers that have been produced using nanotechnology.

Table 1. Summary of the beneficial effects of nanotechnology in comparison to conventionally produced fertilisers

Nanofertiliser	Concentration	Beneficial effect when compared to conventional equivalent
Urea-hydroxyapatite (HAP) coated with wood powder[29]	-	35% less nitrogen release
Nano-coated urea[30]	-	- Pine oleoresin coating: 20% less N_2O emission - Nano phosphate rock coating: 35% less N_2O emission - Nano-ZnO coating: 45% less N_2O emission
Urea-HAP nanohybrid[31]	50 kg ha^{-1}	- Nitrogen release reduced 12 times - 50kg/ha is more effective than 100 kg of conventional urea
NPK-chitosan[32]	10-100 % (foliar sprays)	41% increase in yield
Urea-nano-clay–polymer composites[33]	100 kg ha^{-1}	Dependent on polymer - Nitrogen release rate: 21-25% reduction - N_2O emission: 38-86% reduction
Nano hydroxyapatite (nHAP) [34]	triple super phosphate (TSP)	Seed yield and growth rate increased by 20 and 33%, respectively
Nano calcium carbonate[35]	10 mM	Effects greater than conventional $CaCl_2$ (Root and shoot length, water content, seed germination)
Iron and Magnesium Nanofertilizers [36]	0.5 g L^{-1} + 0.5 g L^{-1}	- Nano Iron: improved the number of pods per plant (10-20%), weight of 1000 seeds, yield and chlorophyll content. - Nano Magnesium: improved the uptake of stem and leaf

There is also a reduction in transportation and application costs due to the lower quantities required for these smart-fertilisers.[37] Importantly, they can be prepared according to the nutrient need of specific crops or to target specific imbalances in soil composition. This provides farmers with the opportunity to further enhance the value of agricultural products.[38] Numerous approaches have been developed to utilize nanotechnology to prepare smart-fertilisers. Smart-fertilisers can be divided into three main categories: nanoscale fertilisers (synthesized nanoparticles), nanoscale additives (nanoscale supplement materials added to bulk products), nanoscale coatings, or host materials (fertilisers with polymer coatings or distributed on porous materials).[39] Nanomaterials with enhanced properties such as zeolite (natural clays)[40-43], hydrogels[44-47], carbonaceous materials (nanotubes, graphene oxide)[48, 49] and polymers[50-53] have been used in studies on slow-release smart-fertilisers.

However, some important limitations to the extensive use of smart-fertilisers should be considered. These include new environmental and unintended health safety issues, such as phototoxicity.[54] In some specific preparation methods of smart-fertilisers such as coating conventional manure with nanopolymer or adsorption of nutrients onto nanomaterials, the consistency in size, shape and composition is an obstacle that can potentially provide poor control of release. Furthermore, if the carrier or the coating of the fertiliser does not degrade or degrades into harmful chemicals, it could result in long-term environmental issues for future crops.[55]

Microfluidic technologies can be used to achieve excellent control over the size and morphology of nano- and micro-capsules and therefore have the potential to overcome production challenges of smart-fertilisers related to achieving uniform chemical and physical properties.[56, 57] In addition, the release rate of the nutrients can be controlled by simply altering the properties of the capsules/support which can be done with ease by changing the preparation procedure (precursor, flow velocity, size, device position).[58] Moreover, the chemical composition of the materials can be modified for specific applications. Furthermore, phase separation in microfluidic devices can create nano-droplets with multiple compartments or multi-layers that can contribute to the encapsulation and controlled release of multiple nutrients for different purposes.[59]

A considerable number of reviews have reported the formation of micro- and nanodroplets made by microfluidic devices. We like to shortly sum up some relevant, typical past reviews and their foci. For example, the fabrication of monodispered droplets and double emulsions was reviewed by Tan et al.[60] Bah et al. reviewed the fabrication and application of complex microcapsules.[61] The preparation of advanced drug delivery systems using microfluidics was summarised by Sanjay et al. and Liu et al.[62, 63] Microfluidics also have important roles in promoting the clinical translation of nanomedicine and it was extensively reviewed by Ahn et al., Colombo et al.[64, 65] Lou et al. and Swider et al. summarized the specific inorganic or polymeric NPs production within microfluidics.[66, 67] Core-shell microparticles generated from microfluidic for a wide range of applications by Galohahi et al. and later a more detailed review on drug carrier by Kashani et al.[68, 69]

To benchmark against this background, our review is first up to date, compiling both past and very recent information. Our review is also holistic, and comprises a good part of the whole subject, while above reviews focus on a fundamental topic or application. More importantly, this review aims to bridge between fundamentals of microfluidics and its applications;

which our group has done for the last 2.5 decades. In this context, the scaling up of micro flows to a relevant industrial scale is pivotal. Thus, we have covered this asset in our review. On another note, real-world applications and their underlying fundamentals must be addressed to lead to an industrial transformation by disruptive technologies, as we have seen happen by the implementation of continuous-flow technology into pharmaceutical process development. In this sense and against the backdrop of a university with long AgriFood research history, we try to give in this manuscript a perspective guided by the application to nanofertilisers and nanopesticides, which we have addressed recently from the disruption by plasma technologies.[70] Those nutrient-related applications rank consistently in the top engineering science applications in major international ranking lists.

2. The challenges of nano-enabled fertiliser production

Two of the most common approaches for creating nano-enabled fertilisers are nanomaterial-supported nutrients and nanomaterial-coated fertilisers. Numerous synthesis routes have already been developed to create nano-enabled fertilizers based on these approaches .[71, 72] However, there are still many challenges to reach their full potential in agriculture. Industries such as cosmetics and food, generally do not require high drop size uniformity, and thus can use conventional techniques for large-scale particle production.[73, 74] However, this is not the case for precision agriculture and nano-enabled fertilisers. Conventional particle fabrication techniques typically generate a broad particle size distribution and sometimes lead to a low encapsulation efficiency.[75, 76] There are few commercially viable ways of preparing particles with a controlled number of inner cores or to encapsulate different types of inner cores in the same system.[77-79] Conventional preparation of nano-carriers also exhibit a similar problem in the homogeneity of the final products. Furthermore, in nano-enabled fertilisers, the release mechanism of nutrients depends on the properties of the material (e.g., composition and thickness of the coating, affinity with nutrients) and the environmental factors (e.g., temperature, ionic strength, osmolality, pH). Moreover, conventional particle fabrication methods cannot create nanomaterials with different well-defined properties, which limits the ability to elucidate the key parameters influencing nanomaterial performance and design. There are also several other challenges associated with the nanomaterials produced using conventional fabrication methods. The release of nutrients may not synchronize with a plant's nutrient requirement and may be adversely impacted by changes in environmental conditions such as moisture levels, pH, temperature, and microbial contamination. Hence, conventional nanotechnology systems may fail to deliver nutrients as required for different species of plants or different nutrient requirements at each growth stages.[28]

Another direction of applying nanotechnology in agriculture is to synthesize nanoparticles as fertilisers. However, the high energy demand in the production of the nanoparticles obstructs their successful implementation.[80] In addition, the aggregation or dissolution of nanoparticles is another major technical challenge. These phenomena convert nanoparticles into non-nano entities and therefore negate the size-dependent benefit of nanoscale fertilisers. Thus, further research for nanotechnology-based fertilisers is necessary to overcome these limitations. Microfluidic approaches provide promising routes in the preparation of complex morphology multiple emulsion drops with low energy requirement and independent control of:

(i) the dimensions and hierarchical structure of the products;[81-84]
(ii) the formation of multiple cores and multicomponent capsules;[85]
(iii) the rate of drop generation.[86]

3. The development of controlled release conventional fertilisers

Controlled release functions are already designed into many conventional fertilizers so as to improve their performance. This is typically achieved by coating the fertilizers with materials that protect them from mechanical and chemical damage, as well as control their release profile.

Currently, different organic (e.g. neem cake[87], latex[88]) and inorganic (e.g. sulfur[89], gypsum[90], clay[91]) materials are used as coatings for controlled release fertilizers (CRF). Sulphur is one of the most widely used materials for coating fertilisers due to its low water permeability and price. However, sulphur coatings are amorphous, thereby limiting the efficient control of fertilizer release. The performance of sulphur-coated fertilisers can be enhanced by further coating them with a layer of polymer to produce polymer-cum-sulphur coated fertilisers.[92] Polymers such as polyurethane and alkyl resin are often used commercially for directly coating urea to produce CRF.[28, 93]

In general, fertilisers are submerged in a polymer solution and stirred for a specific time. The coated fertilizers are then removed and dried. Another way to produce CRF is to spray the fertiliser surface layer-by-layer with the coating solution in a rotary tank or a fluidized bed reactor. A solid shell is formed by drying, crystallization, or polymerization to obtain the final products.[53, 94]

3.1. Rotary tank for preparation of coated fertilisers

Spray drying is often used to generate core-shell structures for controlled release fertilisers due to its ability to rapidly and economically produce dried materials at a large-scale. Rotary drum spraying is also commonly used to produce fertilisers containing controlled-release nutrients.[95] The initial granular fertilisers are loaded inside a rotary tank/pan and the coating is then sprayed onto the granules. The period of spraying the coating material is the most important process parameter. As the fertiliser's surface is wetted by contacting the solution, the particles may collide with each other to form liquid bridges which will become larger clumps after drying. Furthermore, to achieve a uniform thickness of the coated layer for the entire batch, a large amount of coating material must be utilized.[53] To

avoid clumping or forming uneven coatings, factors such as the position of the spraying nozzles, rotary speed of the drum, the maximum amount of fertiliser per batch, the tilting angle of the drum, and the processing time have to be taken into consideration. These factors have to be optimized depending on the equipment, fertilisers, and coating materials used.

Polymer-coated fertilisers are commonly produced using the spray coating technique. To be successfully used for encapsulation, the polymer material must have a relatively low cost, be environmentally friendly, and be non-toxic. Several polymers have been shown to exhibit excellent coating properties. Polyvinyl alcohol (PVA) is one of the most suitable materials as it is hydrophilic, biodegradable, and non-toxic. It can be further improved through cross-linking with oxalic acid, glutaraldehyde, or polyvinylpyrrolidone (PVP), which is highly compatible with PVA, as well as being water-soluble, low toxicity and chemically stable.[96, 97] The addition of biochar into polymer coatings has been proven to increase their mechanical strength, prolong nutrient release, and/or increase the degradability of coatings due to its ability to adsorb soil microorganisms.[98-100] As an example, urea-based fertilizers have been successfully coated by composite films consisting of copolymer and biochar (Figure 1), which reduced the rate of nutrient leaching (Figure 2).[100] Chitosan is a natural cationic polymer that can be used as a coating material to formulate controlled-release fertilisers. Chitosan is biodegradable and has the ability to form thin films.[101] Furthermore, it can be used in combination with various natural anionic polymers due to its ability to form electrostatic complexes with them.[102] Although this approach has been widely used for decades, its coating uniformity and reproducibility are still relatively low.[53, 103]

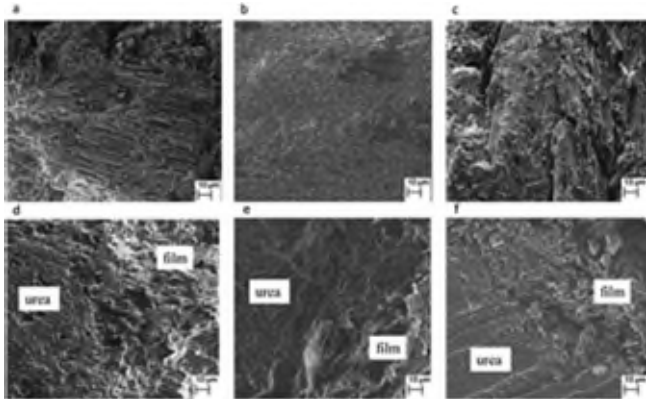

Figure 1. Microscope images for (a,d) maize, (b,e) rice and (c, f) litter biochar-based copolymers coated urea prepared using spray drying in a rotary tank, where (a, b, c) are the surface morphology images (magnification of ×1000) and (d, e, f) are the cross-section views of the coated urea (magnification of ×3000) (with kind permission of Elsevier[100])

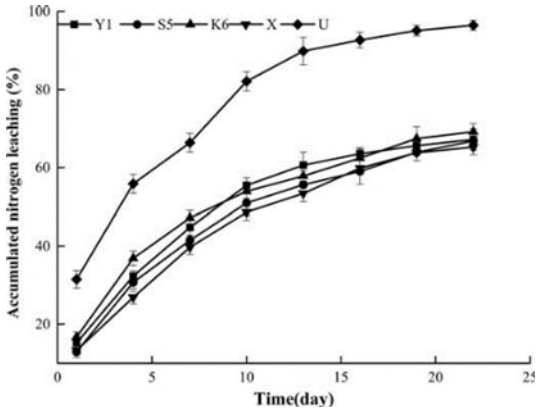

Figure 2. Nitrogen release behaviors in soil: (Y1) maize, (S5) rice, (K6) litter biochar-based copolymers coated urea particles, (X) conventional slow-release urea and (U) pure urea particles (with kind permission of Elsevier[100])

3.2. Fluidized bed reactor

While the rotary pan coating process usually produces shells with rough surface morphology, a lot of pores and defects, coated fertilisers with good coating quality and uniform thickness can be achieved in fluidized bed reactors. Inside the bed column, the granules are first suspended in a fluid-like state using a bottom-up air supply and are then spayed with a coating solution to form a shell.[104-106] The coating material can be introduced into the reactor *via* top spraying, bottom spraying, or submerging inside the bed, as shown in Figure 3.[107]

The swirling bed reactor, where granules are forced to flow in a designed orbit under the influence of an air stream, is considered to be the most reliable equipment for the production of CRF using the fluidized bed method [94]. One instance of applying this type of device is the coating of granular urea with modified corn starch solution.[108] The coating was tested for its ability to act as a physical barrier to prevent nitrogen loss. Poly(acrylic acid) (PAA) is also a suitable candidate for coating urea due to its low cost, biodegradability, and biocompatibility.[109, 110] In some cases, the difference in whether the copolymerization happens before or simultaneously with the coating process can lead to a change in coating properties, as shown in Figure 4.[111] Some other parameters can also affect the quality of the coated fertilisers produced using this approach. The coating thickness depends on the size of the granules and the viscosity of the coating solution.[112] The mass of polymer deposited on the surface is affected by the initial size distribution of the granules.[113] The nozzle injection process also contributes to the quality of the coating in terms of controlling the size distribution of the droplets by changing the injection pressure.[114] However, spray droplets produced at very high pressures may exhibit drifting through the air and splashing from exposed surfaces, which is undesirable for the production of uniform coatings. It is typically necessary to optimize the spray parameters to ensure good coating formation, reduce operating cost, and reduce environmental impacts. Another factor that needs to be optimized is the volume of coating solution as excessive uses may result in large clumps when the granules are dried, as well as leading to de-fluidization of the bed.[53]

ARTICLE

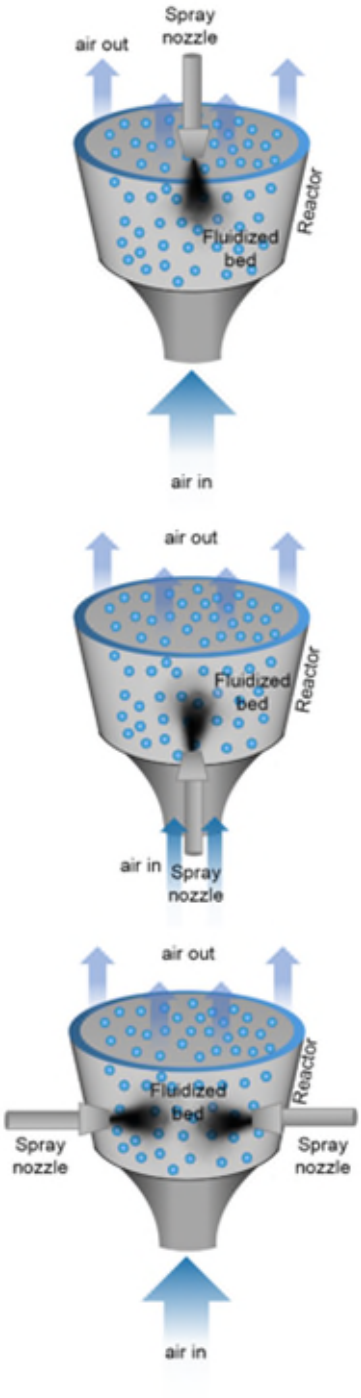

Figure 3. Nozzle positions in fluidized bed reactors: (a) top, (b) bottom and (c) submerged sprayed fluidized bed. (redrawn with kind permission of American Chemical Society [107])

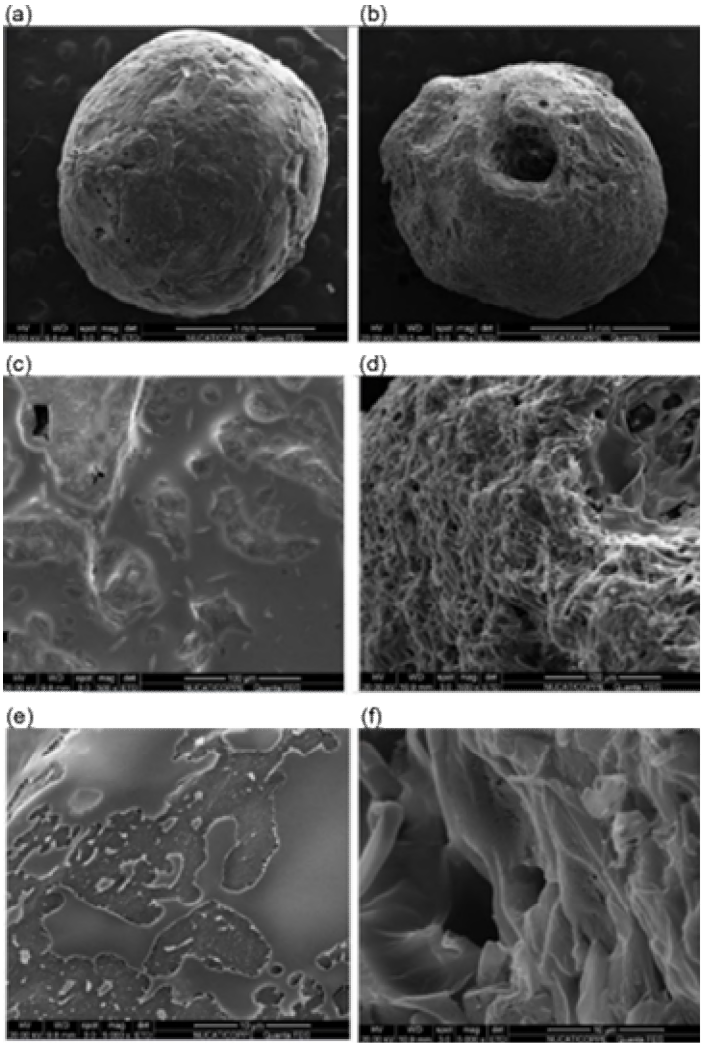

Figure 4. SEM images of coated urea: (a-c) coating polymerization occurred before coating; (d-f) copolymerization and coating occurred simultaneously. (with kind permission of Brazilian Polymer Association [111])

Figure 5. V-star reactor at Chechen State University, Grozny (with kind permission of IOP science[115])

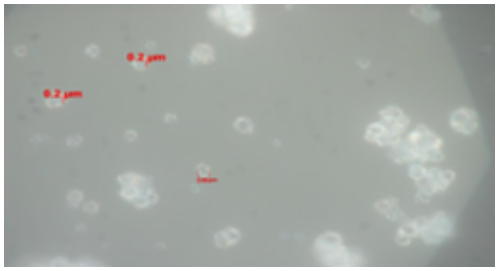

Figure 6. Microscope image of model powder particle with coating using V-star reactor (100x magnification and 0.9 resolution) (with kind permission of IOP science[116])

Table 2. Total content of mineral nitrogen in the soil and the effect on the growth of plant[115]

	Total content of mineral nitrogen in soil (mg/kg)	Biometric indicators of plant depending on the fertiliser applied		
		Height (cm)	Mass of bushes (g)	The leaf area
No fertiliser	17.5	29.0	354	0.35
Non-coated NPK (100g) + biopolymer (20 g)	20.7	35.0	450	0.51
Biopolymer coated NPK (120g)	28.5	46.1	501	0.75

3.3. V-star reactor

Processes such as batch mixing or spray coating can be used to coat fertilisers with a protective outer layer. A so-called V-star chemical continuous flow reactor has been applied to coat conventional NPK fertilisers with biodegradable polyvinyl alcohol.[115] The V-star reactor is a multistage reactor with the parallel stages on a horizontal platform and the final stages act as condensers to allow crystallization and to cool down the product (Figure 5). The coating of model powder particles has been conducted to investigate the efficiency of the V-star reactor.[116] The average size of these coated materials were 206 µm with a coating thickness of 20 µm (Figure 6). As shown in Table 2, the total content of mineral nitrogen in the biopolymer-coated fertiliser is higher than for conventional materials. The application of the coated fertilizer had a positive effect on the growth of plants, with the mass of tops and the leaf area increase nearly 1.5 times compared to the use of non-coated fertilisers.

4. Two types of reported microfluidic nanofertiliser products

Nutrient use efficiency (NUE) is defined as the ability of plants to obtain and transport nutrients in roots and to redistribute them to other parts of the plant.[117] Low NUE is a systemic problem for conventional fertilisers. Hence, farmers tend to use a higher fertilizer input to compensate and achieve good crop yields. This creates other problems such as distortion of the local ecosystem due to fertiliser runoff, increase in energy and material costs for the production of fertilisers, which increase the economic burden on farmers, and obstruct the further development of sustainable agriculture.[118]

4.1. Nutrients on nanosupports

The use of nanomaterials as a carrier for nutrients has the advantages of being safe to users, environmentally friendly and can be tuned to further control the release behaviour. Nutrient carrier nanomaterials can be divided into categories based on their composition and morphology. Five of the most mentioned nanomaterials are nanoclays, mesoporous silica, hydroxyapatite nanoparticles, polymeric nanoparticles, and carbon-based nanomaterials.[117]

Nanoclay consists of silicate platelets with a thickness of approximately 1 nm, which can be separated into two major types depending on their surface charge: anionic and cationic.[119, 120] Nanoclay contains a wide range of materials from montmorillonite[33, 121], zeolite[43] to kaolinite[122, 123]. These materials have been popularly used to create carriers for nanopesticides[119], as additives in food and beverage packaging[120, 124] and medical applications[125]. Nanoclays possess the potential to enhance plant growth, improve NUE, balance nutrient supply, and reduce environmental impacts. These attributes are a result of their ability to protect and provide sustained release of nutrients because of their unique internal structures.[126-128] The nutrients are located between the platelets, which protects them from the environment and controls their release profiles. Hydroxyapatite (HA) is another material that is suitable for the creation of nano-enabled nutrient delivery systems. Because of its presence in human and animal hard tissues, HA is biocompatible and also known as “bone mineral”. As both Ca and P are present in its structure, it has the potential to deliver these nutrients to crops. Furthermore, its high surface area and formation of a moderately strong bond with urea make HA a particularly suitable material for the slow release of nitrogen.[29, 31, 129] Mesoporous silica and carbon-based materials can also be utilized as fertilizer carriers due to their large porosities and surface areas. However, demanding synthesis methods obstruct both materials from becoming popular as nutrient delivery systems.[130-132] Chitosan is commonly explored for its potential as a fertiliser delivery system because of its low cost, high abundance, and good biodegradability. Indeed, NPK-loaded chitosan nanoparticles have been developed and shown to be effective for the protection and controlled delivery of fertilizers.[32, 133,

[134] Various other natural and synthetic materials have also been researched for their potential to create nanoenabled delivery systems for fertilisers.[30, 135] Indeed, this is a highly active area and it is likely that new nanomaterials will be developed in the future with novel or enhanced performance.

4.2. Microcapsules

Microencapsulation is the process of generating microspheres or capsules with a size of 1-1000 μm by using a polymeric membrane to coat or entrap a core material (which may be solid, liquid, or gaseous).[136] These microspheres or capsules are engineered to release their core at a controlled rate over long periods.[137] This versatile technology also allows the manipulation of the microcapsule's properties, and thus has been used in many fields, such as medicines, chemistry, and the food industry.[138-142] The controlled release of nutrients, when loaded in biodegradable microcapsules, is beneficial to the fertiliser industry as it contributes toward the goal of sustainable agriculture by producing fertilisers enhanced performance.[143]

Table 3 provides a summary of polymers that have been applied for controlled-release purposes in agriculture. Resins and thermoplastics are most commonly used as organic polymer membranes for slow-release fertilisers but they are expensive and non-biodegradable.[136] Thus, alternative materials are being explored for this purpose.[144] Biomass-derived materials have been widely used for controlled release fertilisers as they are abundant, non-toxic, economically feasible, and environmental-friendly [136]. Chitosan has been extensively used as a support material (*e.g.,* in membranes and granules) for controlled- or sustained-release fertilisers (urea, NPK, $CaH_4P_2O_8$, KNO_3).[145] Lignin is a natural and biodegradable polymer derived from lignocellulosic biomass. It slowly decomposes from dead vegetation and eventually becomes part of soil humus, which increases the photosynthesis production of the plant.[146] Hence, urea with lignin coating has high nutrient efficiency because the nutrients are slowly released as lignin decomposes and the coating itself becomes a nutrient for the soil.[147, 148]

The decomposition of a polymer in soil can be due to chemical and/or biological processes, with chemical degradation typically occurring before microbiological degradation. Hydrolysis is the most common nonbiological degradation process of polymers (e.g., polyesters, polyanhydrydes, polyamides, polycarbonates, polyurethanes) and has been extensively reviewed in the literature.[149-151] Furthermore, the most important factors affecting the chemical degradation of polymers (such as polymer type, copolymer type, pH, and temperature) have also been reviewed previously.[152] Microbial polymer degradation typically consists of two main steps.[153] The first step involves depolymerisation (or chain cleavage) under the action of extracellular enzymes and normally occurs outside the organism. The second step involves the transport of small oligomeric or monomeric fragments into the microbial cells, which then undergo mineralisation.[153]

The selection of suitable materials for the preparation of microcapsules intended for utilization as fertilizers is critical for their performance. In particular, NUE is an important factor that needs to be considered when choosing these materials as it is considered to be a crucial standard to evaluate the quality of fertilisers. Environmental compatibility, production costs, and potential for toxicity must also be considered. Many of the studies mentioned above focused on naturally occurring materials as they are environmentally friendly, safe, and inexpensive. However, environmental risk assessment, toxicity studies, and economic analyses are critical for the successful commercial application of these materials. Future studies should focus on establishing release mechanisms and kinetic models as they have largely been ignored in previous research, even though this knowledge will affect the dosing and applying frequency to meet a plant's need.

Table 3. Typical polymers used in slow/controlled-release materials

Polymers	Agrochemical	Ref
Chitosan	Urea KH_2PO_4 NPK $CaH_4P_2O_8$ KNO_3 Hexazinone ($C_{12}H_{20}N_4O_2$) 2-chloro; 4-chloro-phenoxyacetates (2CPA and 4CPA)	154-160
Cellulose	NPK Urea 2-chloro; 4-chloro-phenoxyacetates (2CPA and 4CPA)	161-163
Alginate	Paraquat ($[C_6H_7N)_2]Cl_2$) 2-chloro; 4-chloro- phenoxyacetates (2CPA and 4CPA)	160, 164
Natural gum	KH_2PO_4 NPK KNO_3	156, 165, 166
Polyurethane	Urea Bifenthrin ($C_{23}H_{22}ClF_3O_2$)	163, 167

5. Characteristics of microfluidic nanofertiliser products

To answer the question of whether microfluidics can be a useful tool in the production of nanofertilisers, we first take a brief at what this technology has achieved over the years since it was emerged in the scientific literature in 1997.[168] The evolution of microfluidic flatform can be divided into two distinct stages corresponding to two decades of this technology coming to existence[169]: the first stage of functional droplet manipulation and application in simple chemical and biological problems[170-174]; and the second stage of exploration in complex applications in the field of biology, chemistry and material sciences using high-throughput microfluidic systems[175-178]. Table 4 summarises the application of microfluidic platforms in various fields. The general advantages of all microfluidic systems include low sample volumes, high droplet generation frequencies, the ability to access sub-millisecond mixing time and the possibility of creating

multifunctional systems that overcome problems that affect the efficiency of continuous flow systems (e.g. slow mixing, surface-molecule interactions, Taylor dispersion).[179]

With the goal of preparing nano-enabled fertilisers using a microfluidic platform, the following routes can be implemented: (i) flow focusing of microjets to yield nanojets giving nanodroplets by flow instability (e.g. Rayleigh-Plateau instability)[180-184], or (ii) formation of nanoemulsions by self-organisation through tailored surfactants [185-187]. In addition, nanocoating techniques for microdroplets are known, since the term nano-enabled fertilisers can also be implied to the nanocoating of particles. Here, the coating thickness is on nanoscale and triggers different responses to the stimulus in soil (e.g. pH, temperature, microorganism). These nanocoatings can be generated layer-by-layer using microfluidic platforms in the following way: (iii) microencapsulation of nanodroplets [188], (iv) nanocoating of micro-nanoparticles prepared using microfluidic platform[189, 190]; (v) multilayers of nanocoating for protecting and controlled release of core[191].

Table 4. Summary of application of droplet-based microfluidics in pharmaceutical processing.

Type	Material	Size	Application	Ref.
Microdroplets/ Microcapsules	PVA, PCL, PEG	23-47 μm	Pharmaceutical/Therapeutic proteins	192
	Ca-alginate	60-467 μm	Pharmaceutical/Therapeutic proteins	193, 194
	PAH, PSS, FITC, PLLA, PLGA	50-80 μm	Drug carriers	195-197
	Poly-urea	27-35 μm	-	198
	PEGDA	~100 μm	Cardiovascular therapeutics	199
	Chitosan, Alginate	~100 μm	Drug carriers, nanoparticles encapsulation	200-202
Nanodroplets/ Nanoparticles	PAM	20-32 nm	Gastro-intestinal tract	203
	Lipid NPs	20-50 nm	Pharmaceutical applications	185
		~80 nm	Therapeutic siRNA	186
	PLGA-PEG	25-200 nm	Drug discovery and clinical translation	204
	PGLA-cholesterol	103-106 nm	Anticancer drug	205
	Chitosan/TPP NPs	~119 nm	Drug carrier	206
	PLGA NPs	< 200 nm		207
	Metal core-shell nanoparticles	35-85 nm	-	208
	Biocompatible colorant-loaded nanoparticles	~12 nm	Natural color drinks	209
	PGLA NPs coated with lipid, liposomes	~40 nm	-	210

5.1. Ease of droplet formation

Conventional emulsions are colloidal dispersions consisting of two immiscible liquids, with one of them being dispersed in the other in the form of small droplets.[211] Oil and water are the two most common immiscible liquids used to formulate emulsions. Emulsions are thermodynamically unstable systems because of the positive free energy associated with the oil-water interface, which is a result of the hydrophobic effect. As a result, they usually have to be made kinetically stable by adding emulsifiers or texture modifiers. Two kinds of conventional emulsions are widely used in commercial practice, which differs in the relative arrangement of the two immiscible liquids: water-in-oil (W/O) emulsions and oil-in-water (O/W) emulsions.[212-215] However, it is also possible to create more sophisticated structured emulsions such as water-in-oil-in-water (W/O/W) or oil-in-water-in-oil (O/W/O), which are known as multiple or double emulsions, with enhanced functional attributes. Emulsions can be used as delivery systems themselves or they can be used as templates to form other kinds of delivery systems, *e.g.,* by solidifying one or more of the phases. The structure of emulsions plays an important role in the preparation of microcapsules for the protection and release of fertilizers.[77, 192, 216]

The droplets in multiple emulsions can be divided into four major groups: single-cored, multi-cored, Janus, and multiple-compartment, as shown in Figure 7.[211] Single-core emulsion droplets have an onion-like configuration consisting of a core and one or more layers, with each component being immiscible with its neighbours. For instance, two (double-emulsion drops), three (triple-emulsion drops), four (quadruple-emulsion drops), five (quintuple-emulsion drops) or more layers can be included. However, the greater the number of layers, the higher the production costs. Multi-cored emulsion droplets contain a controlled number of multiple inner cores (two or more). The inner cores can be comprised of similar or distinct liquids, with each liquid playing a different role. Janus droplets have two physically and chemically distinct domains. These droplets can either be used as an inner core or an outer shell. Multiple-compartment droplets are those with high levels of complexity in their

configuration, such as high-order emulsions with different inner and middle drops.

Microfluidics refers to a group of fluid manipulation technologies that utilize a network of channels with dimensions of tens to hundreds of micrometers.[217] Microfluidic devices can produce a wide variety of droplets with distinct morphologies and are divided into several categories. Based on the main liquid propulsion principle, the microfluidic systems are divided into five major groups: capillary-based, pressure-driven, electrokinetic, centrifugal, and acoustic microfluidic platforms.[218] However, pressure-driven microfluidic systems are the most commonly used for chemical synthesis because of their ease of control and flexible design. Herein, we review several widely used pressure-driven systems in preparing microfluidic emulsion droplets.

Typically, batch methods are used for the large-scale production of structured emulsions because of their low cost, speed, and high capacity (Figure 8). However, it is important to optimize the processing parameters during the development stage e.g., materials, volumes, flow rates, stirring speeds, and processing times.[218-221] Microfluidic methods may have advantages over traditional batch methods since they can carry out several different processes in parallel or sequentially, thereby facilitating the formation of complex emulsion structures, as well as having the potential to be fully automated.[222-225]

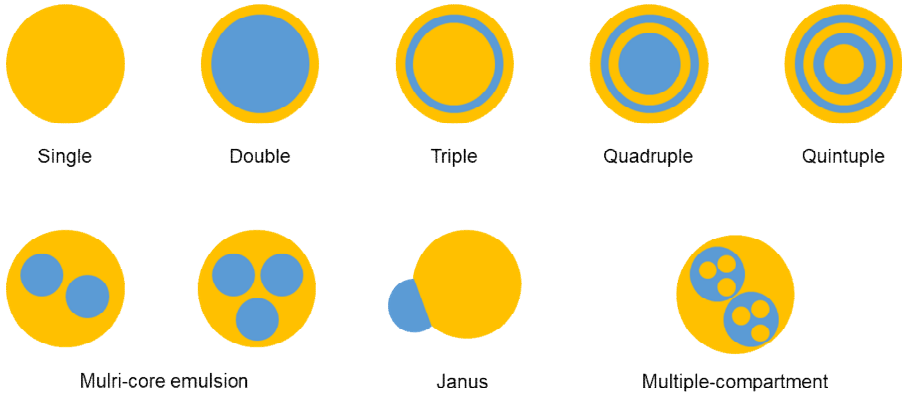

Figure 7. Classification of emulsion droplets based on configurations and orders (with kind permission of Multidisciplinary Digital Publishing Institute[211])

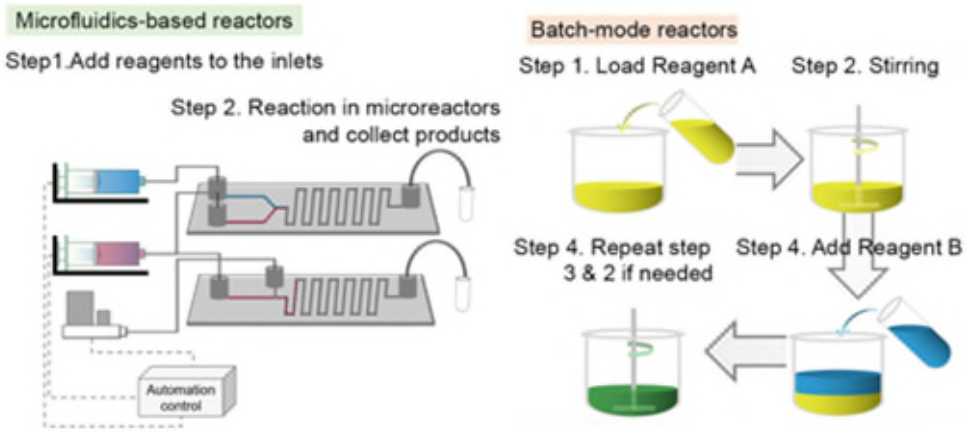

Figure 8. Schematic illustration of (left) microfluidics reactors and (right) batch-mode reactor (redrawn with kind permission of The Chemical Society of Japan[221])

Table 5. The comparison between microfluidic reactors and batch reactors [219]

	Microfluidic reactors	Batch reactors
Tunable parameters	Wide range	Narrow range
Reaction/process time	Seconds or less	Hours – Days
Precise control	Yes	No
Reproducibility	Medium - High	Low
Automation	Advanced	Given
Consumption of reagents	Low	High
Scale-up probability	Low – Moderate	High
Cost	Low cost at high performance	Low cost at large quantity
Harsh conditions	Yes	No

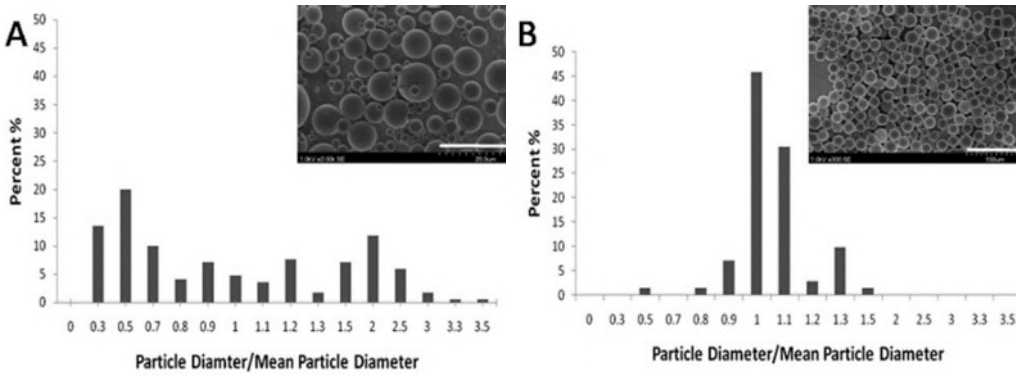

Figure 9. Size distribution and SEM image of (A) polydisperse silica microspheres generated from a shaken bulk emulsion (the scale bar is 20 µm) and (B) silica microspheres generated by a monodisperse microfluidic device (the scale bar is 100 µm) (with kind permission of American Chemical Society[226])

A comparison between reactors operated under microfluidic and batch modes is summarized in Table 5.[219, 222] Microfluidic reactors possess many superior properties when compared with conventional batch reactors. These include, among others, continuous-flow process with constant product quality over time, rapid heat and mass transfer, low volume of fluids, high surface-to-volume ratio and predictable laminar flow. They also require a very low consumption of reagents which benefits reactions involving expensive materials. In addition, microfluidic reactors operate in a confined environment, and thus are suitable for operating reactions under extreme conditions. On the other hand, a potential disadvantage of microfluidic devices is that it is more difficult to produce the large quantities of materials required for many commercial applications, including fertilizers. This problem may be overcome by using multiple microfluidic devices in parallel.

One of the most significant features of microfluidic systems is their ability to generate monodispersed droplets. Figure 9 illustrates the comparison of the particle size distribution of silica microspheres produced by conventional and microfluidic methods.[226] The droplets obtained from the conventional method have a broad range of sizes, whereas those obtained using the microfluidic device have a very narrow range. The monodisperse droplets produced by microfluidic devices would lead to more reliable functional attributes, such as controlled release profiles.

5.1.1. T-Junction microfluidic devices

T-junction devices are the most commonly used microfluidic system in the preparation of emulsion droplets from immiscible fluids. They usually consist of one or more cross-flowing channels of continuous and dispersed phases. T-junctions are classified based on the position of the fluid flows (Figure 10). The mode where the dispersed phase is introduced from a side channel into the main channel of the continuous phase is called cross-flow.[227, 228] In contrast, the mode where the continuous phase is fed from the side channel is called perpendicular-flow. The interaction of the two streams of immiscible fluids in T-junction devices generates shear forces that lead to droplet formation. Previous studies have shown that parameters such as flow rate ratio, injection angle, interfacial tension, viscosity ratio, density ratio and the hydrophobic/hydrophilic properties of the channel affect droplet generation and properties.[229, 230] For instance, the diameter of droplets can be modified by controlling the fluid properties, flow conditions, and the contact angle at the location where the two phases interact. The position where the droplets detach can change between the corner of the T junction and downstream in a jet-kind mode when the flow rate ratio is altered. Furthermore, the shape of the droplet is based on the injection angle and this can also result in a parallel flow without droplet formation (Figure 11).

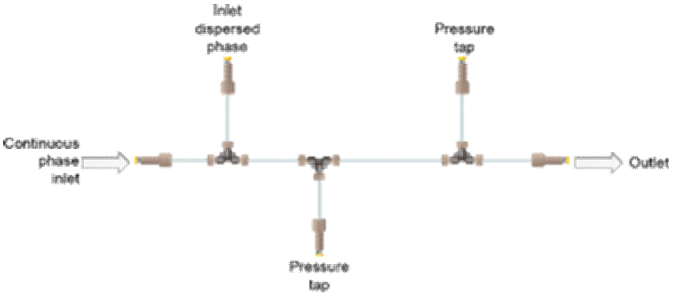

Figure 10. Sketch of a cross-flowing T-junction microfluidic system (with kind permission of Elsevier[229])

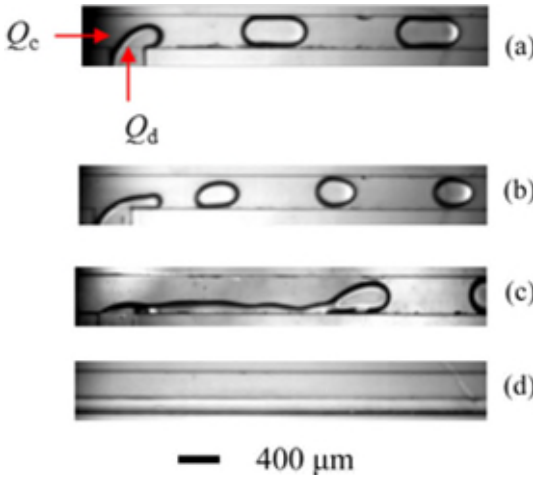

Figure 11. Representative flow patterns of fluid in T-junction channel: (a) slug flow; (b) droplet flow; (c) jet flow; (d) parallel flow (with kind permission of Elsevier[229])

5.1.2. Co-flow microfluidic devices

A simple co-flow microfluidic device consists of a capillary inserted in a tube or another capillary as shown in Figure 12a.[231, 232] This simple structure is most suitable to produce monodispersed droplets where the dispersed phase is inserted through a smaller inner capillary into

the continuous phase moving around the capillary. The position of the break-up of the jet to form droplets depends on the regimes of the inner fluid. The droplets will be formed near the tip of the capillary in the dripping regime caused by a low flow rate of the dispersed phase (Figure 12b). When the flow rate of the dispersed phase increases beyond a limit, the inner fluid begins to jet into the continuous fluid along with the formation of drops downstream through a necking process (Figure 12c).[233] The average size of droplets can be easily controlled by adjusting operating parameters (e.g., flow rate ratio of both phases, the viscosity of the continuous phase, the inner diameter of the capillary).

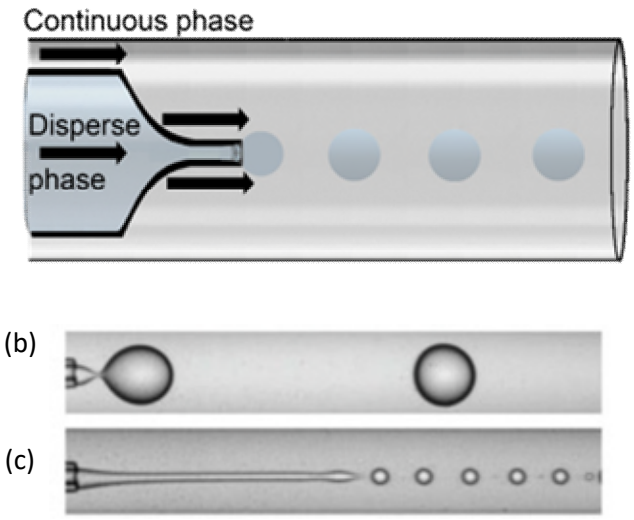

Figure 12. (a) Illustration of a co-flow microfluidic device for emulsion generation (with kind permission of Elsevier[231]). Image of droplets in(b) dripping regime and (c) jetting regime in co-flow microfluidic devices (with kind permission of American Physical Society[233])

5.1.3. Flow-focusing microfluidic devices

A flow-focusing geometry is another design commonly used in microfluidic devices to produce droplets [234]. In the first set-up, the dispersed and continuous phases are introduced from two opposite ends of the same outer capillary tube.[231] As they collide at a specific position, the outer fluid causes the inner fluid to hydrodynamically flow focus through the inner narrow tapered capillary tube and the droplets are formed in the inner channel (Figure 13a). The second set-up consists of two channels that intersect to form a cross-shape, as shown in Figure 13b.[184, 235] The continuous and dispersed phases are injected into the side and central channels, respectively. Drops can form immediately as the dispersed phase enters the inner capillary for the first option and at the intersection for the second option under the dripping regime or it can occur further downstream under the jetting regime. This phenomenon allows the size or shape of the droplets to be tailored for particular applications.

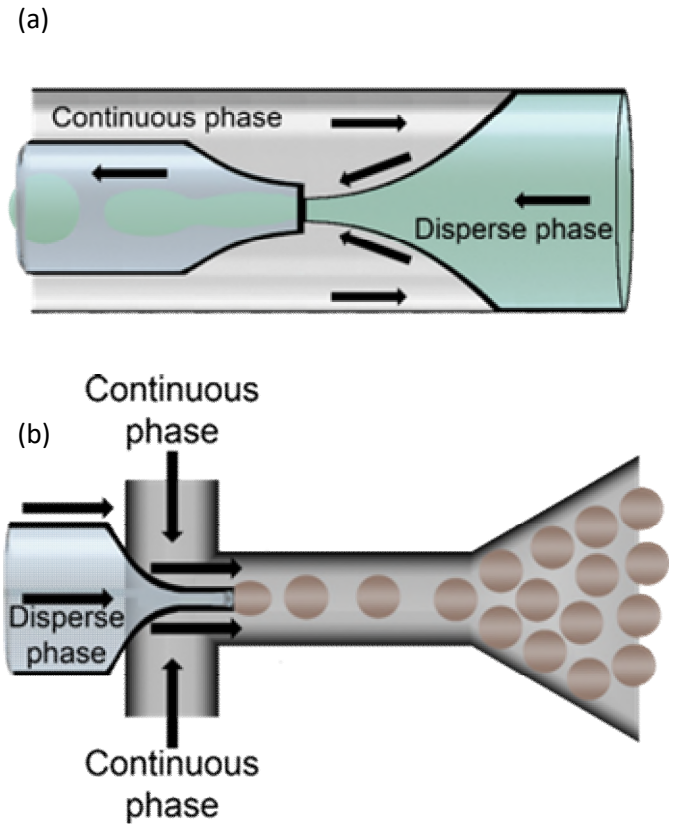

Figure 13. Illustrations of flow-focusing microfluidic devices for making droplets with the different set-up: Opposite flows (a) and intersect flows (b)

5.1.4. Combination

The combination of different types of microfluidic systems or a series of the same system can be used for the formation of emulsions with complex hierarchical structures.[236] These multiple emulsions are utilized for specialized applications such as the encapsulation and release of materials in cosmetic, pharmaceutical, and food applications. One of the most commonly used designs is the combination of both co-flow and flow-focusing in the preparation of double emulsions (Figure 14). The device consists of two end-to-end positioned circular capillaries within an outer capillary. Three fluids flow through the device in a specific direction. The inner and middle fluids flow in the same direction while the outer fluid flows in the opposite direction, which creates a flow-focusing mode. A set of two co-axially arranged capillaries in a tube also allows the production of double droplets.[237] Multiple encapsulations can also be performed using a microfluidic system that consists of a series of co-flowing or flow-focusing layouts. As shown in Figure 15, two sequential co-flow geometries are positioned coaxially for the optimum performance. The advantage of this set-up is the ability to prepare complex emulsion structures by simply adding more stages.

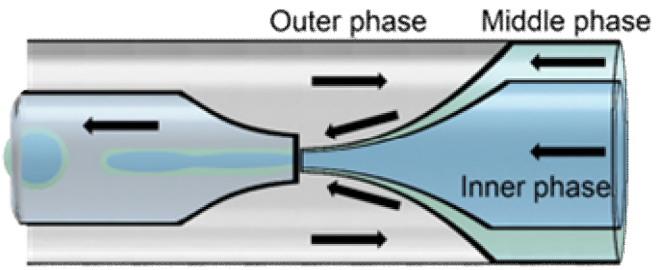

Figure 14. Illustration of a microcapillary device that combines co-flow and flow focusing

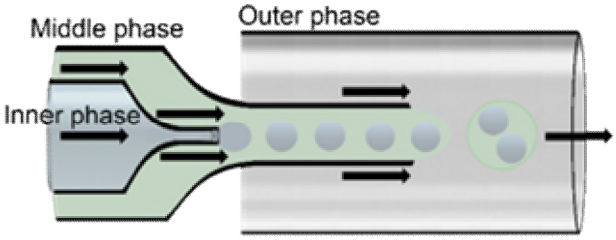

Figure 15. Illustration of a microfluidic device consisted of two sequential co-flow emulsion generators

5.1.5. Micromixing

The common layouts for micromixers in the laboratory scale are the Y-mixer inlet with winding channels (Figure 16) and the spiral-shaped microchannel (Figure 17). Mixing in microfluidic devices relies primarily on chaotic advection and molecular diffusion, which can be tuned by changing the contact surface and the diffusion path between the inlet fluids.[219, 234, 238-240] The highly predictable laminar flow in micromixers allows a fast and controllable mixing process that is ideal for handling reactions with rapid kinetics or unstable intermediate products.[234, 241] During the reaction process, micromixers also allow the addition of reactants at desired time intervals. Thus, they provide the ability to temporally monitor and control the reactions.[242, 243] Reactions can be performed under isothermal conditions as the small dimensions of microfluidic mixers (between 10 and 400 µm) facilitate rapid heat transfer and control [244-246]. When dealing with limited resources, biological and chemical analysis and screening can benefit from the small interval volume required for reaction in micromixers.[234] Furthermore, from the safety-related perspective, the small interval volume of hazardous substances and chemical reactions is significantly less dangerous than in conventional mixing equipment.[242]

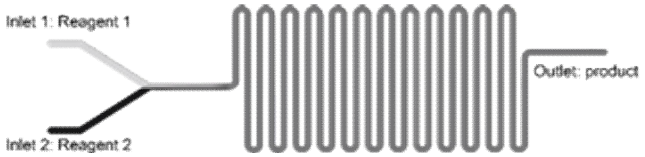

Figure 16. A simple design for laminar-flow microreactor

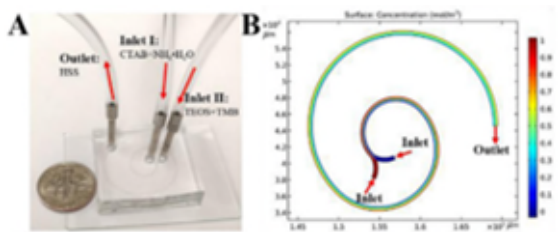

Figure 17. Spiral-shaped laminar-flow microreactor (with kind permission of Elsevier [240])

5.2. Membrane fine-tuning

5.2.1. Membrane thickness modification

The thickness of the shells in emulsion-based delivery systems can be controlled to obtain the release profiles required for specific applications. Hence, there is a need for simple techniques to adjust the shell thickness, such as controlling the jetting regime in microfluidic systems.[247] The jetting regime is produced by simply changing the flow rates of the inlet fluids. Hence, this mechanism allows the control of the dripping instability to break the jet of the fluids and generate multiple emulsions at a desirable position within the device. Figure 18 illustrates the difference in forming an emulsion under normal conditions (a) and jet regime conditions (b). Normally, due to dripping instability in both junctions, the double emulsions would be produced in a two-stage process where the inner and outer drops are formed subsequently in the first and second junction of a microfluidic device (Figure 18a). However, by causing the inner phase to jet, the double emulsion can be formed in one step at the second junction (Figure 18b).

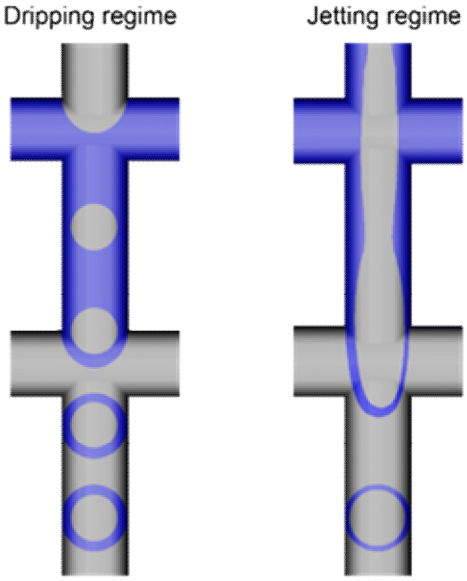

Figure 18. Illustration of a double flow-focus microfluidic device for double emulsion generation in dripping regime (a) and jetting regime(b)

The transition between the two-stage and one-stage formation process can be quantified by measuring the pinch-off location of the drops. At a low flow rate, there are two distinct dripping instabilities in the junctions, and the pinch-off locations of the inner and middle phases are different. As the flow rate is increased, the inner phase jetting causes the drops to pinch off at the same place, as shown in *Figure 19a*. Utilization of the jetting regime enables the fabrication of emulsions with thin shells, which cannot be achieved using the normal two-step process (*Figure 19b*). This is because the flow conditions in the one-step process allow the dripping of emulsion drops to occur. Higher-order multiple emulsions can be created in one-step using the same concept, e.g., a device capable of forming triple emulsions is shown in *Figure 20*. In this case, the jetting fluids break and produce multiple emulsions as the cycle progresses.

Aside from changing the flow rates of the fluids, controlling the height of the tapered region of the injection channel can also affect the size of the generated droplets.[248] In this case, the fluids are injected into the microfluidic device as shown in Figure 21. The breakup and formation of double emulsions are affected by the competition of the capillary and shear forces acting on the outer phase.[248] By altering any parameters that affect the capillary force (e.g., interfacial tension and tip dimensions) or the shear force (e.g., viscosity and flow rate) one can control the size of the droplets produced. As shown in Figure 22, the size of the double emulsion drops increases with decreasing flow rate or increasing tip height.

The shell thickness of the double emulsions can also be controlled by changing similar parameters. For instance, it was reported to decrease from 7.4 to 4.7 µm when the flow rate was increased from 3 to 5 mL h^{-1}, as shown in Figure 23.[248] However, increasing the height of the tip allowed the device to be operated at a lower volumetric ratio of the middle to the inner phase (see insert of Figure 23) and thus reduced the shell thickness.

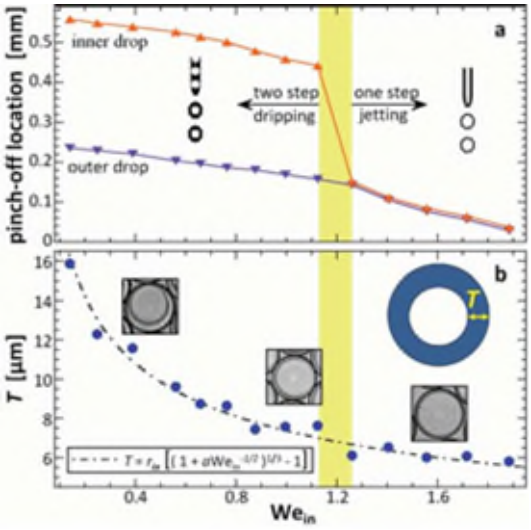

Figure 19. The pinch-off locations of the inner and outer jets (a) and the effect on the shell thickness (b) (with kind permission of Royal Society of Chemistry[247])

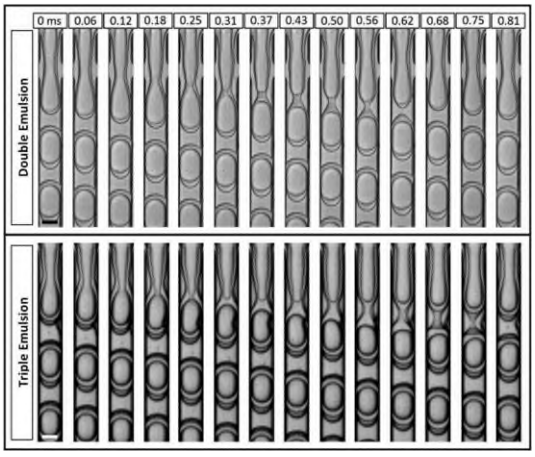

Figure 20. One-step formation of multiple emulsions (with kind permission of Royal Society of Chemistry [247])

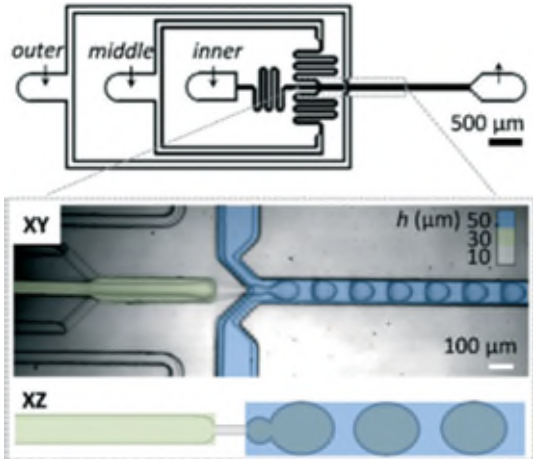

Figure 21. Microfluidic device for generation of double emulsion drops with thin shells. The device contains three different heights (shown by the different colors) (with kind permission of Royal Society of Chemistry[248])

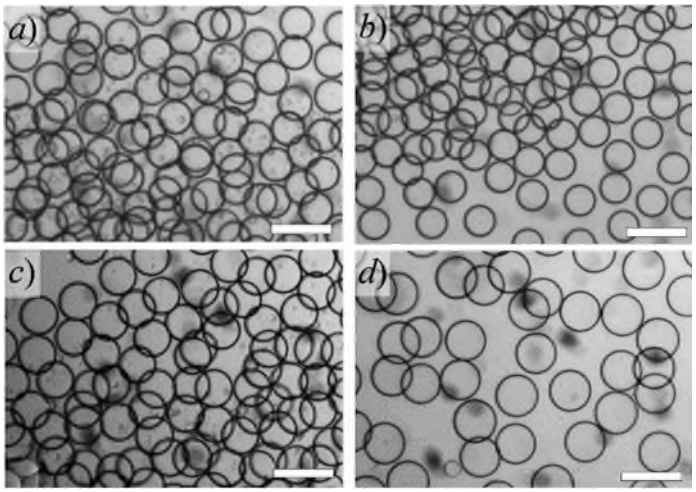

Figure 22. Optical microscope images of double emulsion drops generated from difference in the flow rates of the inner, middle and outer phases of (a) 1, 0.4 and 3 mL h^{-1} and (b) 1, 0.4 and 4 mL h^{-1} and tip sizes of (c) 20 µm and (d) 40 µm. Scale bars are 200 µm (with kind permission of Royal Society of Chemistry [248])

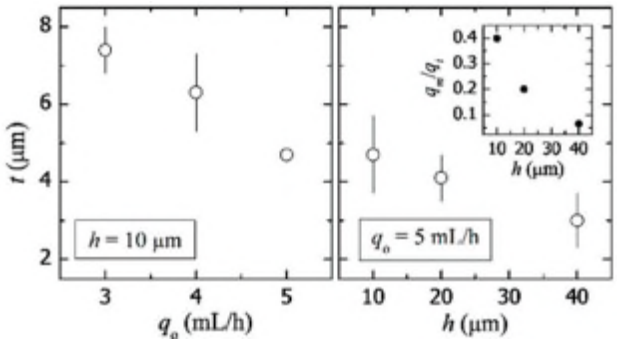

Figure 23. The effect of flow rate (left) and the height of the tapered region (right) on the thickness of the membrane (with kind permission of Royal Society of Chemistry[248])

Based on the difference in the density of the cores and the shells, the shell thickness can be reduced by passing the droplets through constrictions in the channels. As the core's density is lower than that of the shell, it travels through the constrictions faster, forcing the oil

towards the tailing end of the drop. The accumulation of oil breaks up and forms single emulsion droplets (red circles) when it contacts the channel walls, as illustrated in Figure 24a. The shell thickness reduction was tested in two cases, which are the incorporation of the constrictions into the device and the re-injection of emulsions into another series of microfluidic channels. The incorporation of more than three constrictions further increased the hydrodynamic resistance of the channel compromising the process of forming double emulsions in the device. Thus, the reduction efficiency was not as effective as the re-injecting the emulsion drops into a new device with constrictions (Figure 24b).

Usually, the dimensions of the microchannels are adjusted to control the size of the droplets produced without the need to alter the properties of the fluids. But this is time-consuming and challenging for large-scale commercial applications. Yet, this bottleneck can be overcome by utilizing the difference in osmotic pressure between the inner and outer phases.[249] Capsules prepared by solvent evaporation such as PGLA double emulsions are most suitable for this approach. These microfluidic droplets are first generated using a microchannel device with a salt solution of a given concentration as the inner phase. The emulsions are then transferred into a glass cuvette which is later filled with a salt solution of a different concentration (e.g. NaCl). The droplets either shrink or swell due to the diffusion of water out of or into them caused by the difference in electrolyte concentration between the two phases. After the drop had reached equilibrium, the capsule is formed by removing the organic solvent in the oil phase (Figure 25).

The effect of inner and outer salt concentrations on the droplet size is illustrated in Figure 26. The inner droplets shrink if the salt concentration in the inner phase is lower than that in the collection solution and swells in the opposite situation. After 2 hours of osmotic annealing, from the initial inner diameter of approximately 150 µm, the inner phases were reported to reach their equilibrium size and the final microcapsule diameter ranged from around 80 to 300 µm (Figure 26).

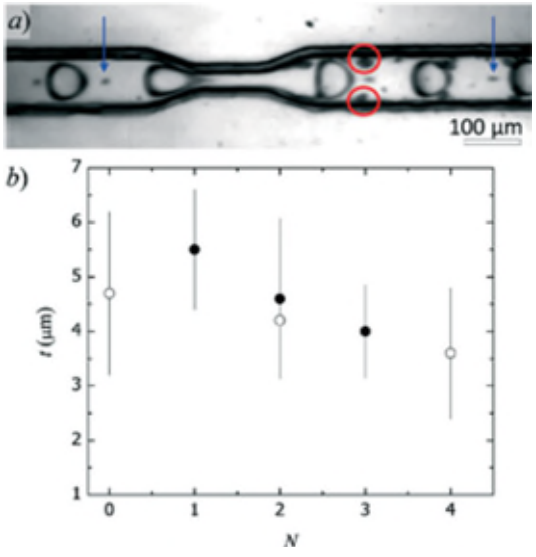

Figure 24. (a) Optical microscope image of constrictions to reduce the shell thickness of the droplets. Removed oil droplets are shown by red circles; satellite droplets resulting from the production are indicated by blue arrows. (b) Effect of the number of constrictions on shell thickness. (with kind permission of Royal Society of Chemistry[248])

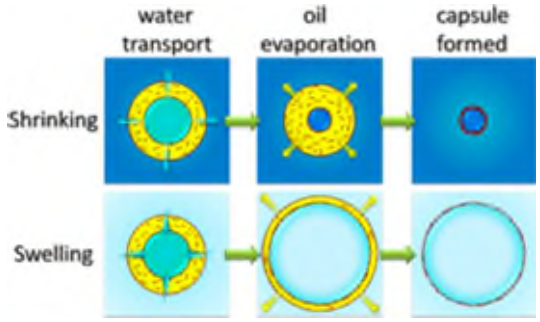

Figure 25. Schematic illustration of tuning the size of double emulsions and microcapsules by osmotic annealing (with kind permission of American Chemical Society [249])

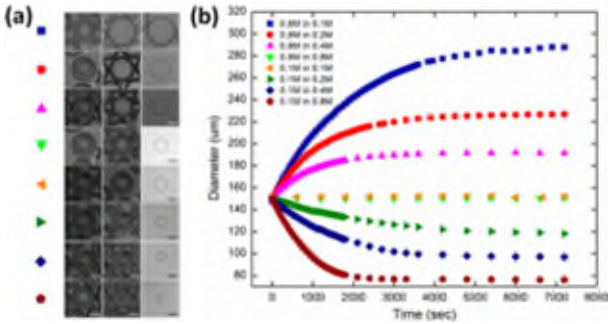

Figure 26. The effect of osmotic pressure on PLGA microcapsules: (a) microscope images of PLGA microcapsules under different osmotic pressure and (b) the diameter changes of the inner droplets under osmotic annealing (b) (with kind permission of American Chemical Society[249])

5.2.2. Membrane solidification

The stability and retention/release characteristics of microcapsules produced from multiple emulsions can be improved by solidifying one or more of the phases inside them. Currently, there are four commonly used methods for shell solidification: polymerization, solvent evaporation, freezing, and dewetting.[250] The selection of a particular solidification method depends on system composition and the requirements of the final application.

Polymerization. Polymerization involves the covalent crosslinking of monomers or oligomers dispersed in one or more of the phases of an emulsion droplet to create a shell (Figure 27a). Heat triggering utilizes a thermal initiator to produce radicals to activate monomers. However, this process may promote the coalescence of some oil droplets at high temperatures. Light triggering overcomes this disadvantage and is the easiest route to initiate the polymerization process. A photo-initiator is typically used that produces radicals when exposed to UV irradiation (Figure 28). It is important to select an appropriate precursor and crosslinking method as this determines the functional characteristics of the shells formed (Table 6). The robustness of the shells formed, as well as the short processing times required to create them, has meant that polymerization has been widely used for shell solidification.

Solvent evaporation. Solvent evaporation is a process whereby a volatile solvent initially located in the middle phase of an emulsion droplet diffuses into the continuous phase or vaporizes into the environment.[251] As a result, the material in the middle phase is concentrated and forms a solid shell (Figure 27b). This means solid shells can be formed using polymers that can dissolve in volatile solvents, such as poly(lactic acid) (PLA)[58] and poly(lactic-co-glycolic acid) (PLGA)[197]. The size of the inner core can be altered by changing

the osmotic pressure of the surrounding medium, when the consolidation process is happening. However, this method requires a long lifetime of the emulsion drops as it is a relatively slow process. The stability of the multiple emulsion can be improved by the adsorption of a molecular surfactant or colloidal nanoparticles onto the interfaces to form a barrier against coalescence until the solidification process is completed. The solvent evaporation method produces densely packed shells with high mechanical stability but low chemical resistance. However, it can be utilized in certain applications, as it can be beneficial for chemical triggered release of the inner phase [252]. This method also has an advantage over polymerization in its ability to produce ultrathin shells.

Freezing. This method utilizes the transition of a material from a liquid to a solid state to form a solidified shell. It, therefore, requires the utilization of materials with appropriate melting behaviours, such as hydrocarbons or other lipids that have freezing points in the range of 30-50°C.[250] During emulsion formation, the system is kept at a temperature above the freezing point of the middle phase so that the molten fluid can flow through the channels in the microfluidic device and form a liquid shell. After emulsion formation, the system is then cooled below the freezing point to solidify the shell (Figure 27c). This type of microcapsule can serve as a delivery system with temperature-triggered release properties. However, shells prepared using the freezing method often have relatively poor mechanical stability, which can result in the leakage of encapsulants due to the formation of pores and cracks, which may limit the application of this method in some cases.

Dewetting. The dewetting process uses a mixture of two distinct organic solvents, one with good volatility and the other with poor volatility, containing either lipids or amphiphilic polymers for the middle phase to form microcapsules with a molecular bilayer membrane. Interfacial energy is minimized as amphiphiles are aligned at both the inner and outer phases. The solvent with higher volatility rapidly diffuses to the outer phase leaving the solvent with lower volatility. The hydrophobic parts of the amphiphiles which remain in the oil phase are pulled together as the quality of the solvent decreases. Upon contact, the two monolayers overlap to form a bilayer as shown in Figure 27d. The bulb is formed from the expelled oil drop from the middle phase of the emulsion and it can either remain or completely separate from the core leaving a single bilayer on the interface.

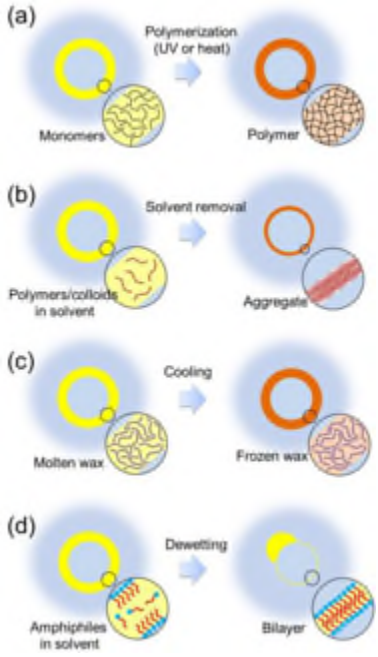

Figure 27. The schematic images showing the process of shell solidification: (a) polymerization, (b) solvent-evaporation (b), (c) freezing, and (d) dewetting (with kind permission of Royal Society of Chemistry[250])

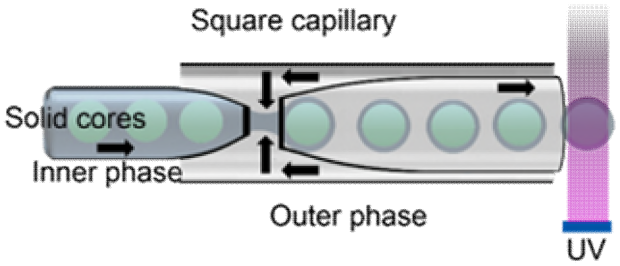

Figure 28. Schematic illustration of microfluidic system with UV polymerization

Table 6. List of some monomers used in UV polymerization

Monomers	Coating properties
Tripropylene glycol diacrylate (TPGDA) [253-255]	Rigid shell
Trimethylolpropane triacrylate (TMPTA) [256]	
Ethoxylated trimethylolpropane triacrylate (ETPTA) [257]	
1,6-hexanediol diacrylate (HDDA) [258]	
Ethylene glycol phenyl ether acrylate (EGPEA) [259]	Elastic shell
Poly(ethylene glycol)diacrylate (PEGDA) [260, 261]	Hydrogel shell
Poly(N-isopropylacyamide) (PNIPAm) [262]	Temperature-responsive shell
Poly(acrylamide-co- carboxyethyl acrylate) [263]	pH sensitive shell

5.3. Nanodroplets formation

The formulation and manufacturing of nanodroplets have been widely studied using multiple conventional preparation processes (e.g. high-pressure homogenization[264, 265], high-speed mechanical agitation[266, 267], sonication[268, 269]), each with their pros and cons in terms of operation, cost, yield, consistency, and size distribution.[270]

Microfluidics is also a candidate technology for the preparation of nanoscale droplets. Malloggi et al. used flow-focussing in microfluidic devices to study the generation of simple and multiple droplets.[271] Their object was to generate droplets within the colloidal range and they had successfully obtained droplets whose sizes were between 900 nm to 3 µm. Having implemented a tip-streaming (thread forming) regime in a droplet-based microfluidic platform, Martz et al. have been able to generate populations of primary sub-micrometer droplets, as shown in Figure 29.[181] A very thin thread of fluid is pulled from the tip of the microchannel and subsequently breaks up into a series of droplets with one order of magnitude smaller than the primary thread.[272] Martz et al. reported that the pressure-controlled reagent delivery system is the most important component to maintain the constant flow rates and consistent tip-streaming to produce droplets with diameter of 300-400 nm.[181] Shui et al. obtained a similar diameter of monodisperse droplets using multiphase nano-microfluidics.[273] They used a droplet-based microfluidic that included nanochannels with a height of 100-900 nm and successfully prepared nanodroplets with diameter as small as 0.4 µm. Xu et al. successfully prepared nanodroplets with diameter as small as 200 nm by utilizing tip-streaming regime in flow-focusing microfluidic platform.[183] Recently, Melich et al. have prepared perfluorocarbon nanodroplets (PFC-NDs) in the range of 200-400 nm using a commercially available staggered herringbone microfluidic mixing (SHM) systems.[274] The SHM systems allow the millisecond mixing of surfactant dissolved in organic phase with a water stream which enables the robust synthesis of monodisperse droplets by supressing the mass transport effects that lead to larger and heterogenous aggregation.[185, 274, 275] The size and uniformity of the PFC-NDs was also reported to be fine-tuned by changing the process parameters (e.g. total flow rate, flow rate ratio) and formulation parameters.

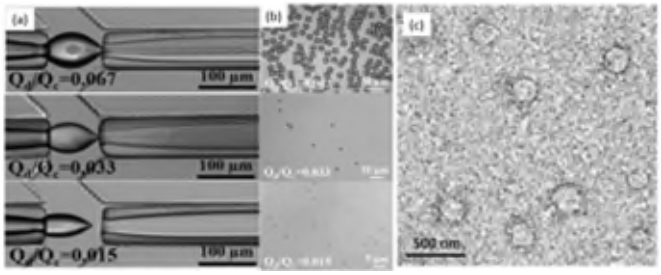

Figure 29. (a) Optical images of the tip-streaming regime in a flow-focusing microfluidic device with different flow rate ratios of oil phase (Q_c) and water phase (Q_d). (b) Optical image of the prepared droplets with a diameter of 10.6 µm, 2.1 µm and 0.7 µm. (c) TEM image of nanodroplet with a diameter of 200 nm prepared using the same device (with kind permission from the Royal Society of Chemistry[183])

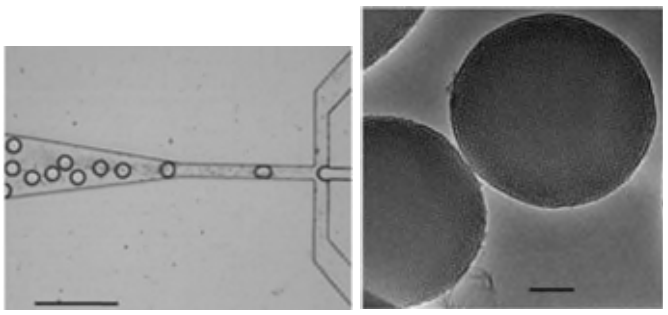

Figure 30. (a) Optical microscopy image of silica droplets precursor in a flow-focusing microfluidic device and (b) TEM images mesoporous silica microspheres (with kind permission of American Chemical Society [226])

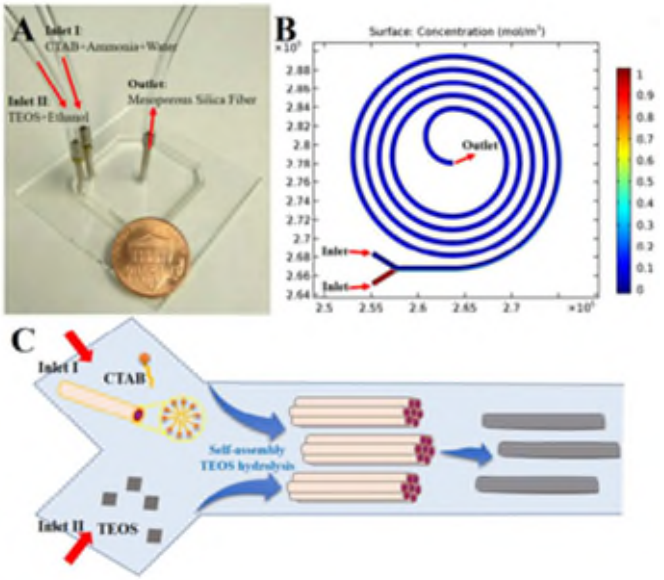

Figure 31. (A) Experimental setup for the microfluidic synthesis of mesoporous silica nanofibers (B) mixing in microfluidic spiral channel simulation using COMSOL. (C) Illustration of the formation of mesoporous silica fibers (with kind permission of American Chemical Society[276])

5.4. Adsorbate fine-tuning

5.4.1. Mesoporous silica particles

Mesoporous silica with different structures (e.g., sphere, ellipsoid, cube) can be prepared using a wide range of methods. However, each of these methods has its advantages and limitations. The evaporation-induced self-assembly (EISA) method uses various types of surfactants and block co-polymers to synthesize well-ordered thin silica films and particles.[277] However, the dimensions of the mesoporous silica particles produced are usually inconsistent. Mesoporous silica fibres can be synthesized using electrospinning and hydrothermal treatments, but they often have low yields, high energy requirements, and poor reproducibility [278-281]. Microfluidic systems provide a straightforward and promising platform for the synthesis of monodisperse mesoporous silica particles.

A flow-focusing microfluidic device can generate monodisperse drops that can act as templates and reactors for producing particles from synthetic or natural polymers (Figure 30a). Monodisperse mesoporous silica particles with highly uniform

pore sizes can be prepared in these systems utilizing the EISA and solvent evaporation methods (Figure 30b).

Different morphologies of mesoporous silica can also be prepared using microfluidic devices, such as fibre structures. Figure 31 illustrates a spiral-shaped microfluidic reactor used to synthesis silica fibres. The ammonia-catalysed hydrolysis and condensation of TEOS using CTAB as a structuring agent can be performed using this microfluidic design to produce mesoporous silica.

As shown in Figure 32, mesoporous silica fibres with average diameters of approximately 130 nm can be obtained at the outlet of microfluidic reactors. The mesoporous channels on the fibres are well-aligned with each other (Figure 32F). The production of mesoporous silica fibres using a microfluidic reactor can be achieved in less than 4 seconds due to the fast reaction kinetics involved.

Different types of functional nanoparticles can be added into mesoporous silica particles due to the flexibility of microfluidic reactors. For instance, Fe_3O_4 nanoparticles have been fabricated using a coprecipitation method and then mixed with the reagent inlet to allow the generation of magnetic mesoporous silica (Figure 33).[240] This strategy can also be applied to produce other kinds of nanoparticles e.g., silver nanoparticles or quantum dots.

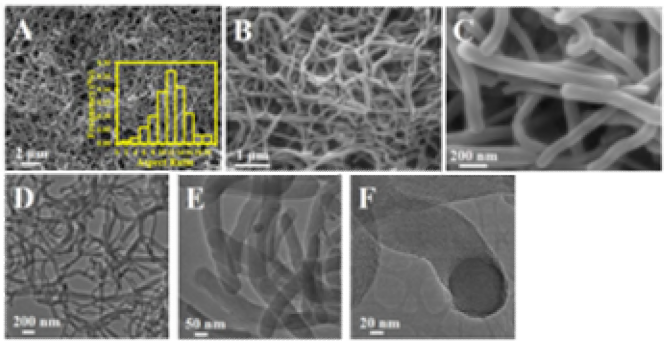

Figure 32. (A-C) SEM images and (D-F) TEM images of mesoporous silica nanofibers (with kind permission of American Chemical Society[276])

Figure 33. TEM images of (i) Fe_3O_4 and (ii) silica sphere-magnetic nanoparticle (SS-MNP); (iii) magnetic separation behavior of SS-MNP under an external magnet (with kind permission of Elsevier[240])

5.4.2. Hydroxyapatite

Hydroxyapatite (HAp) nanomaterials can also be produced using conventional methods and microfluidic devices. Conventional methods include sol-gel procedures[282-285], hydrothermal syntheses[286-288], solid-state reactions[289, 290] and direct precipitation of aqueous solutions[291-293]. Although these methods provide a good strategy for the preparation of hydroxyapatite nanomaterials with enhanced bioactivity, mechanical, and surface properties, the control of the morphology of these materials still remains a challenge. Microfluidic systems can be used for the rapid synthesis of HAp with less reagent consumption and more controlled morphologies.

Possessing the ability to separate each droplet and to allow the addition of new reactants by diffusion through the middle shells, double droplets have been utilized as microreactors for the synthesis of HAp nanopowders.[294] Double emulsion droplets containing calcium and phosphorous precursors have been prepared using a glass capillary microfluidic system (Figure 34a). To trigger the HAp formation reaction, the pH was adjusted by adding an alkali (e.g., ammonium hydroxide) to the continuous phase. As shown in Figure 33b, the reaction happened immediately after the addition of NH_4OH resulting in instantaneous precipitation. After 91h, the solid precipitated structure remained intact while the droplet exhibited swelling due to the difference in the osmolality of the inner drop and outer phase (Figure 34c). At this point, the shell got thinner and would likely burst to release the precipitates.

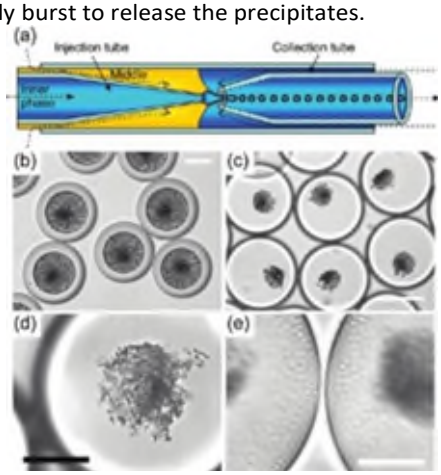

Figure 34. (a) Illustration of the glass microfluidic device for double emulsion droplets formation. (b-e) Optical microscope images of double emulsion drops: (b) immediately and (c) 91 h after the addition of NH_4OH solution. Optical microscope images of (d) a hydroxyapatite particle aggregate formed and (e) oil shells at higher magnification (with kind permission of American Chemical Society[294])

The same concept of using droplet fusion as a basis to form microreactors for the preparation of HAp have been implemented in simple double T-junction microfluidic reactors (Figure 35a).[295] Droplets containing phosphorus and ammonia precursors were formed and then interacted with calcium through droplet fusion (Figure 35c). Droplet fusion allows precise mixing of reagents at a desirable position in space and time by having different components in different droplets.[296] As shown in Figure 35d, the HAp powder obtained contained bundles of monodisperse needle-like crystals.

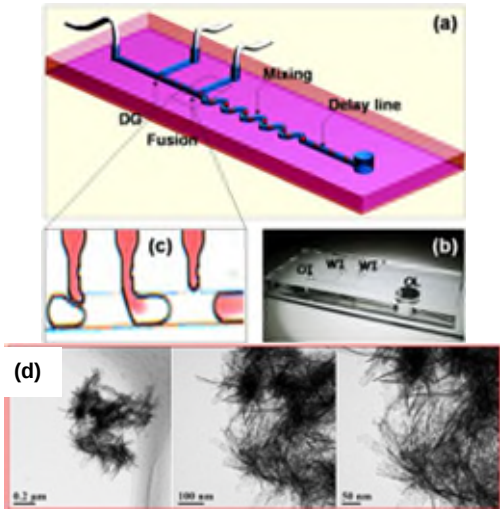

Figure 35. (a) Sketch and (b) prototype of the microfluidic fusion chip. (c) Microscope image of the droplet fusion process. (d) TEM images of dried hydroxyapatite powder (with kind permission of IOP science[295])

In general, different designs of microfluidic systems can be used to create particles with different shapes. Figure 36a illustrates a microfluidic system composed of two associated Y-junction chips designed for the synthesis of HAp nanorods.[297, 298] The morphology of HAp was controlled by the addition of surfactants (CTAB) as the micelles were converted from spherical into rod-like shape when the surfactant concentration surpassed the critical micellar concentration. The obtained HAp nanorods corresponding to the CTAB micelles with a narrow size distribution were confirmed by TEM analysis (Figure 36b).

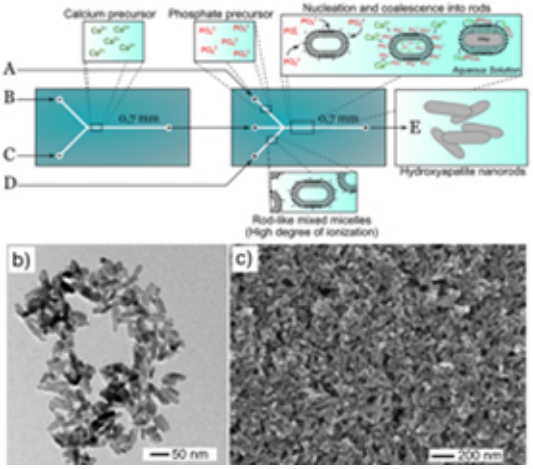

Figure 36. (a) Illustration of the microfluidic system for preparing HAp nanorods, (b) TEM image and (c) SEM image of hydroxyapatite nanorods (with kind permission of American Chemical Society[297])

5.5. Sustained/triggered release behaviour

Microfluidic devices can be designed to create fertiliser formulations with sustained-release characteristics, which allows precise control of the nutrient concentration in the media nourishing the crops. As an example, microfluidics has been used to prepare emulsions consisting of an inner aqueous phase encapsulated by a solidified poly(lactic-co-glycolic acid) (PLGA) membrane.[197] These microcapsules were stored in a phosphate buffer solution (pH=7.4) for several months to observe their release behaviour. The most important factor that impacted the release rate of the capsules was the membrane thickness (Figure 37). For instance, 13%, 9%, and 6% of the initial inner phase of the capsules was released within the first 24 hours for membrane thicknesses of 70, 105, and 105 nm, respectively (Figure 37f). After 90 days, more than 85% of the microcapsules with a thickness of 70 nm released the aqueous core (Figure 37b). It took 120 days and 150 days to release 80% of those with a membrane thickness of 105 and 150 nm, respectively (Figure 37c,d). These results highlight the ability to tune the release characteristics of microcapsules by altering their internal architecture.

Poly(lactic acid) (PLA) membranes can also be used to create sustained-release formulations due to their biodegradable characteristics. For instance, the inner cores of microcapsules containing thin PLA shells were slowly discharged over months when suspended in aqueous surfactant solutions (Figure 38).[58] This process can be accelerated by creating a high osmolality difference between the core and the phase. In Figure 39, capsules with a higher osmolality dispersed in distilled water started to release the inner phase within a day. After 61 hours, all the interior core had escaped.

Another desirable feature for some applications is to have smart capsules that can trigger the release of an active agent under some targeted conditions, such as a specific pH, ionic strength, temperature, or enzyme activity range. For example, microfluidic prepared polystyrene (PS) capsules have been shown to exhibit triggered release behaviour in a liquid plasticizer stimulus.[252] A mixture of inert linear alkanes and toluene (10, 50, and 100 wt%) in oil was prepared to investigate the trigger release behaviour of the microcapsules. The adsorption of toluene caused the membrane to be fluidized and the capsule structure was restored to that of a double emulsion. The inner phase was driven out of the capsule through this localized surface defect. The encapsulated cargo was rapidly released (< 1 sec) after the membrane burst after it was exposed to a pure toluene stimulus (Figure 40a). The toluene within the oil mixture was then reduced to 50 wt%. The inner phase of the capsules was gradually released over a 75 s period and the capsules exhibited shrinkage during this process (Figure 40b). The capsules achieved a slower and more sustained release of the encapsulant when the toluene content was reduced further to 10 wt%. In this case, the fully released duration was 12 minutes and the capsule membrane deflated (Figured 40c).

An experiment on the effect of pH on the triggered release of microcapsules was conducted by Lee et al.[197] Microcapsules with 105 nm thickness were used to study this influence and were separately suspended in three solutions with different pH values (pH 2, 7.4 and 9). As shown in Figure 41, the capsules in the acidic and alkaline medium had a faster release rate than those in pH 7.4. After 50 days, only 45 % of capsules were released in pH 7.4 while approximately 82% and 90% were released in pH 9 and pH 2.

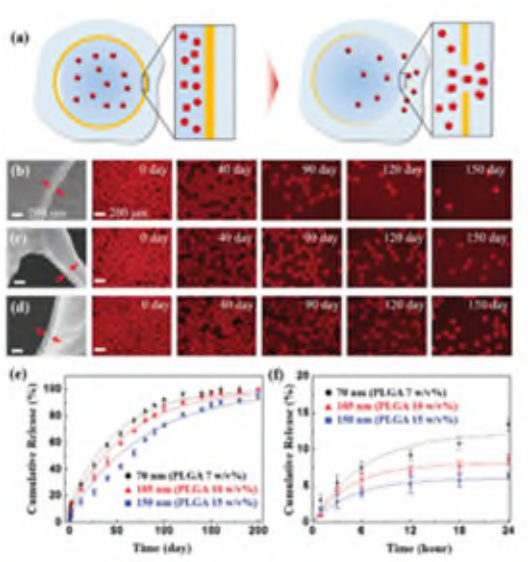

Figure 37. (a) Illustration of the release of the core through a hole formed by degradation of the thinnest part on the membrane. (b-c) SEM images of membrane cross-sections with fluorescence microscope images showing the release of the inner phase with the membranes average thicknesses of (b) 70, (c) 105, and (d) 150 nm. Cumulative release of inner phase from microcapsules with membrane thicknesses of 70 nm (black circles), 105 nm (red triangles), and 150 nm (blue squares) in (e) 200 d and (f) 1 d (with kind permission of (with kind permission of Wiley VCH[197])

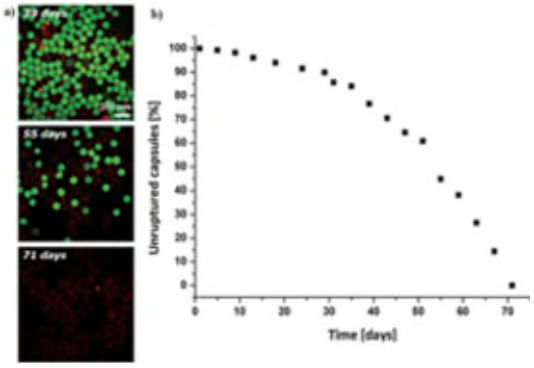

Figure 38. (a) Microscope images of microcapsules after 33, 55 and 71 days. (b) Fraction of unruptured capsules as a function of time (with kind permission of Royal Society of Chemistry[58])

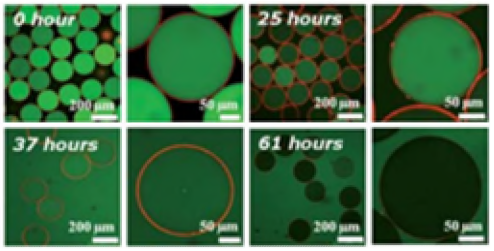

Figure 39. Microscope images of microcapsules dispersed in water after the preparation, 25 hours, 37 hours and 61 hours (with kind permission of Royal Society of Chemistry[58])

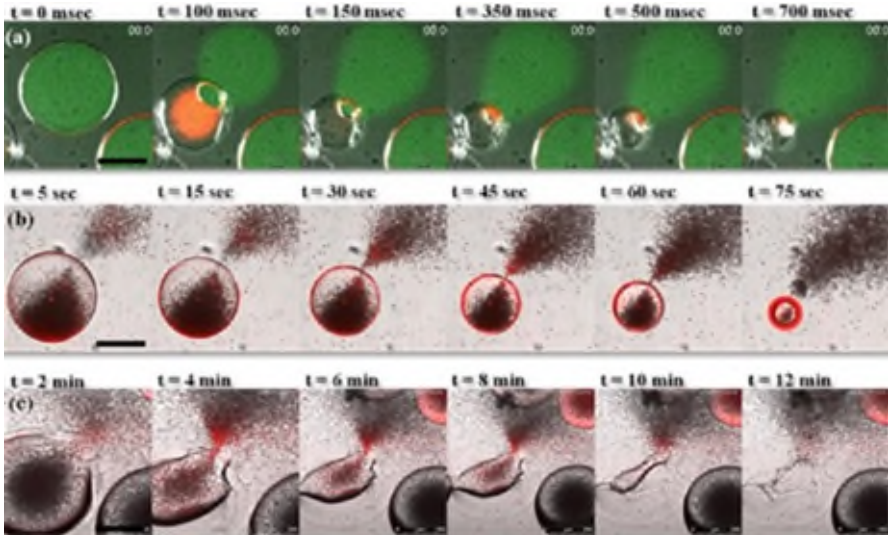

Figure 40. Time-lapsed microscope images showing release behavior of capsules exposed to different concentrations of toluene stimulus: (a) 100 wt %, (b) 50 wt %, and (c) 10 wt % (with kind permission of American Chemical Society[252])

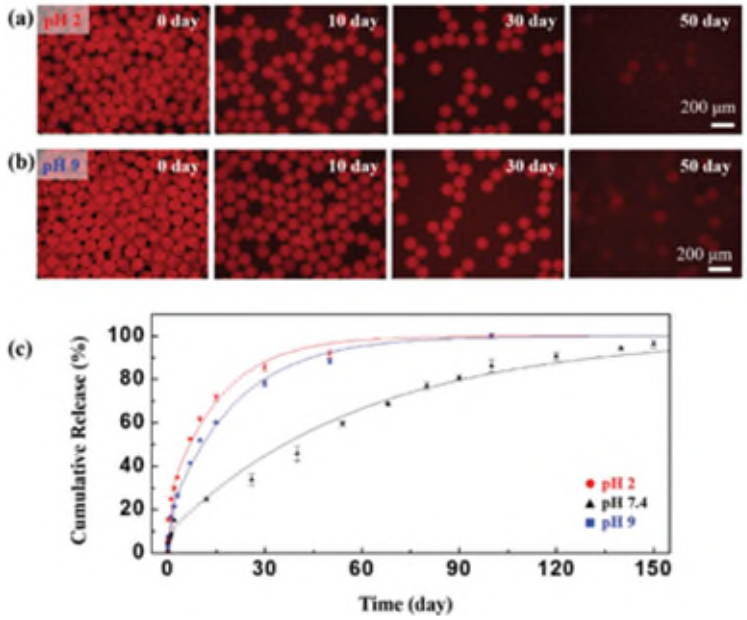

Figure 41. Fluorescence microscope images of microcapsules prepare by a co-flow microfluidic system with 105 nm thick membrane at (a) pH 2 and (b) pH 9 and (c) the cumulative release of inner phase from the microcapsules at pH 2, 7.4 and 9 (with kind permission of Wiley VCH [197])

5.6. Multi-core and non-spherical core hierarchy

Crops usually require a variety of nutrients and thus farmers tend to apply different types of fertilisers at different stages throughout the year. This process is time-consuming and the majority of nutrients usually runoff before they can be absorbed by plants. Owing to the ability to generate multiple core capsules using microfluidic devices, it is possible to prepare multi-functional fertilisers consisting of many nutrients, which only need to be applied to the soil once and still provide enough nutrients for plants.[299] This is a significant advantage of microfluidic-prepared capsules over the usage of nanosupports for nutrient adsorption as the concentration of nutrients can be precisely controlled from the beginning and it can be easily changed by altering process parameters.

Microcapsules with solid cores have been prepared using a T-junction microfluidic system that can create single and double capsules.[300] When the dispersed phase is injected at a fixed flow rate, the number of cores depends on the flow rate of the oil phase. As shown in Figure 42a(i)-(v), at a low flow rate of the oil phase, no breakup of the dispersed phase happens before the second core enters the channel creating droplets with two solid cores inside.

Microfluidic encapsulation allows the incorporation of multiple actives that may be incompatible with each other and therefore need to be separated. Alternatively, microfluidic devices can be designed to incorporate multiple actives that need to be released in response to different environmental triggers. As a result, there has been great interest in preparing multicomponent microcapsules using this method. The addition of an injection capillary can be integrated into double or even triple capillary microfluidic devices, with each capillary acting as a transportation channel of different cores (Figure 43a-d). Different combinations of solid cores can be generated, such as A+B (Figure 43e), A+2B (Figure 43f), 2A+B (Figure 43g) by adjusting the flow rates of the fluids in each capillary channel.

Coating non-spherical particles with a uniform shell thickness, which is difficult to achieve using conventional coating methods, while preserving the shape and curvature of the particle surface, can be performed with ease using microfluidic technology. By pulling the particles across the interface of aqueous and non-aqueous phases using magnetic forces in a microfluidic chip, non-spherical particles can be covered with a uniform shell.[301] Figure 44 shows bullet-shape magnetic particles passing through the interface during the coating process.[302] They are covered with a thin film of the aqueous phase and continue to move through the oil phase. Close-up images of the coating process are shown in Figure 45a-c and the coating fluid of the particle is approximately uniform as shown in Figure 45d.

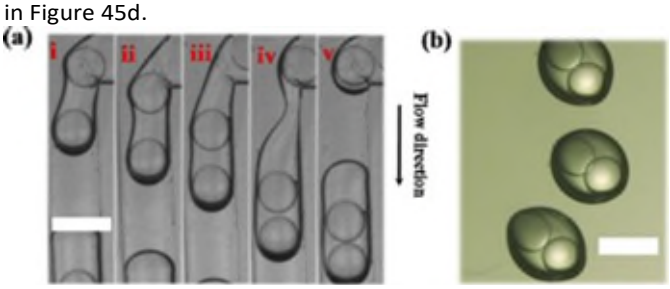

Figure 42.(a) Real-time images of the formation process and (b) optical image of droplets with two solid cores, the scale bar is 1000 μm (with kind permission of Elsevier[300])

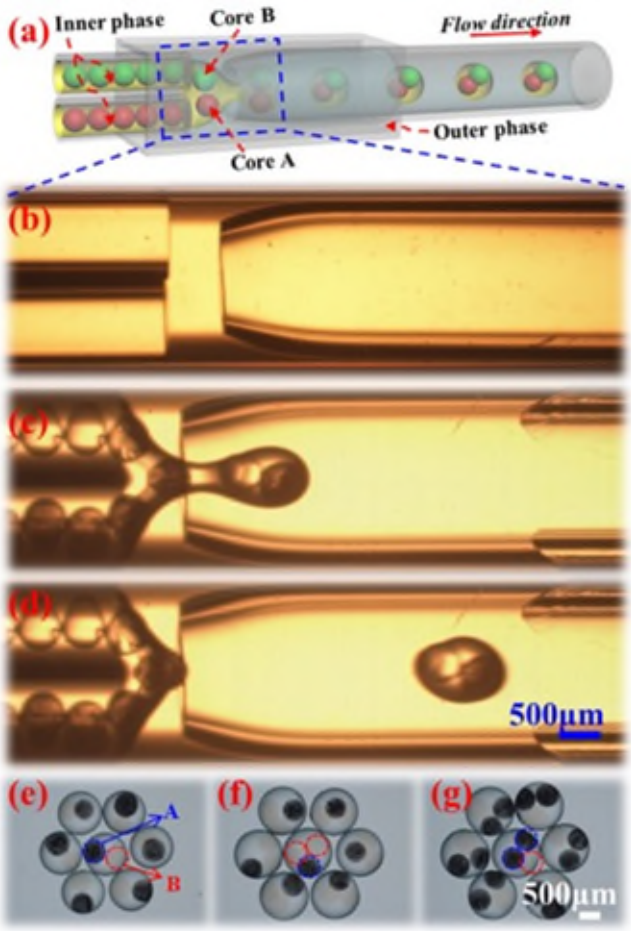

Figure 43. Multi-core encapsulation via parallel microcapillary chip: (a) schematic illustration; (b) microscope photographs of microchannels; (c, d) real-time microfluidic images; (e) combination of A + B; (f) combination of A + 2B; (g) combination of 2A + B (with kind permission of Elsevier[303])

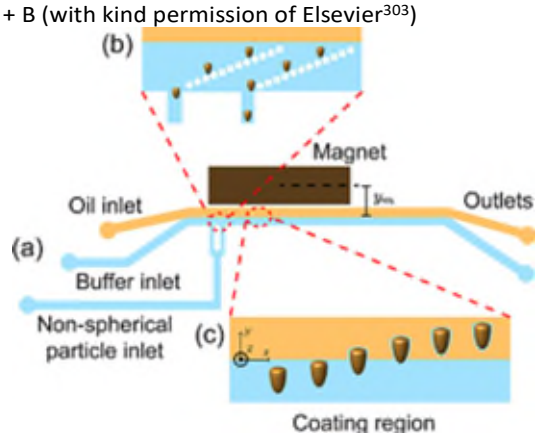

Figure 44. Illustration of the microfluidic device for coating of non-spherical particles using magnetic forces (with kind permission of American Institute of Physics[302])

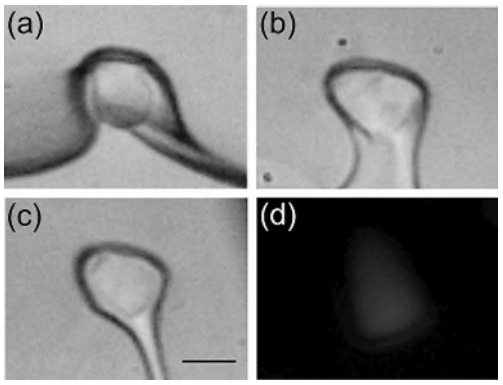

Figure 45. Microscope images of real-time coating of non-spherical particles. (a) The particle reaches the interface. (b) It passes from the aqueous (lower) phase to the non-aqueous (upper) phase. (c) The particle is conformally coated with the aqueous phase. (d) The fluorescent image of the coated particle (with kind permission of American Institute of Physics [302])

5.7. Active droplet-based microfluidic platforms

The active microfluidic platform can be divided based on the energy type: electrical, magnetic, thermal and mechanical.[304] In electrical control, the manipulation of droplet generation can be performed by using electric energy (direct current - DC or alternating current – AC).[305, 306] An electric field was applied on the microfluidic device using embedded electrodes and this will cause charges to migrate and accumulate on the fluids interface. By applying an appropriate distribution of the electric field to control the interaction between surface charges and electric field, we can have additional control of droplet generation.[307] Electro microfluidic platforms can be further divided into constant DC[305], DC pulse[308], low-frequency AC[309, 310], high-frequency AC[306]. Magnetic control applies to the use of magnetism to control the generation, transport, splitting, morphology and position of droplets in microfluidic platforms.[311-315] In general concept, this type of active microfluidics requires the usage of either oil-based or water-based magnetic fluids of suspended magnetic particles with a size less than 10 nm that can be magnetised/demagnetised with the apply/withdraw of a magnetic field either.[304, 311] The implementation of the magnetic field can vary based on the factors including the type of magnet (permanent magnets[311, 316] or electromagnets[317, 318]) or the characteristics of the magnetic field: uniformity (non-uniform[311, 319] and uniform field[316, 320]), direction to the main flow[317] (parallel, inverse polarity or perpendicular), in-plane[316, 318] or out-of-plane[320] of the microfluidic chip. Manipulation of droplets generation by utilising the temperature dependency of the fluid viscosity and interfacial tension is classified as thermal control. It can be divided into localized heating[321-323], or heating the entire microfluidic device[324] with the heat source being heater or laser. Microfluidic platforms where the sound wave is used to control micro- or nanoscale objects or fluids are classified as acoustic microfluidic devices. This type of device has been reviewed in literature[325] with a wide range of applications such as processing of nanoscale analytes[326-329], single-cell manipulation, and analysis[330-332], tissue engineering[333-335].

6. Scale-up strategies of microfluidic reactors for industrial uses

From a technological perspective, microfluidic technology may surpass conventional processes. However, the biggest challenge to applying microfluidic reactors for the industrial production of nanofertilisers is their relatively low throughout put. Assuming a continuous production line, a microfluidic reactor with a single drop generation unit (DGU) with ideal droplet formation characteristics may only give a production yield of a few g h^{-1}. Thus, it would only produce a few 10 kg per year.[336] A real-case fertiliser production plant operates at several 100,000 t a^{-1}. That would translate to millions of microfluidic devices and corresponding equipment such as pumps, which would be cost-prohibitive. The total global demand for nitrogen, phosphorus, and potassium fertilisers use in 2021 is forecasted to be approximately 200 million tonnes.[337] There is therefore a clear need for a proprietary solution for scale-up for droplet-generating microfluidic devices.

The most viable option for scale-up production using droplet generation units must guarantee two levels of structural integration. The first level is to incorporate as many parallel units in one reactor (or chip) as possible to increase the output per pump. The second level is to integrate multiple chips with hundreds of units into a production plant.[338] The common layouts of microfluidic channels for the distribution of fluids into multiple DGUs that preserves the structural integration are tree networks (Figure 46a) and ladder networks (Figure 46b). The tree-type network is more energy efficient in terms of feeding the DGUs. However, if a defect occurs in one branch, the symmetry of the system will be broken and affect the entire droplet formation process. The ladder network offers a design that is more compact and less affected by the random defects in the channel size.

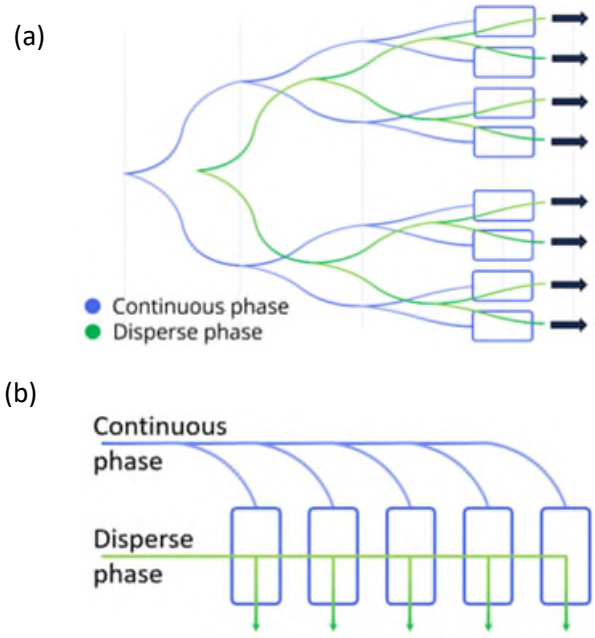

Figure 46. Common layout of microfluidic channels for production scale-up: (a) tree network and (b) ladder network

6.1. Simple droplets formation

Conchouso et al. designed a tree-type (or petal-type) device that consisted of 512 parallel DGUs by stacking multiple layers of DGUs organized in a circular array (Figure 47).[339] Each layer of droplet generation comprised 128 DGUs and was interconnected using through-holes. The minimum dispersity for the devices occurred at 120 mL h^{-1} per layer and four layers can reach disperse phase production rates of 1 L h^{-1}. The droplet size variation was as low as ~6% even though the devices were fabricated with a channel accuracy larger than 4%.

Tetradis-Meris et al. described a design strategy to scale up to 180 cross-junction DGUs for the production of monodispersed emulsions with droplet diameter variations less than 5% [340]. The device was set up using layers of channels stacked on top of each other. The top, middle, and bottom layers are the drop generation layer, continuous phase distribution layer, and disperse phase distribution layer, respectively. The 20 cross-junction DGUs were arranged in one parallel line and there were 9 lines on the top layer. Figure 48 illustrates a strategy for connecting the cross-junction DGUs using a ladder-type network. The two separate drainage channels (one for each phase) allow the assistance of the start-up and clean-up process.

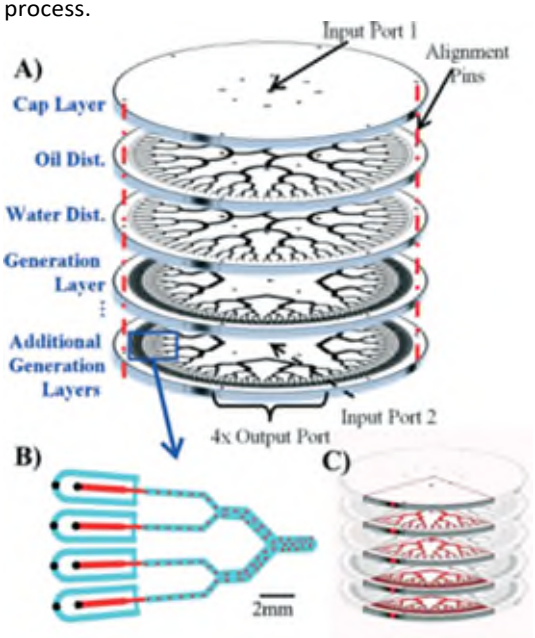

Figure 47. (A) The stackable configuration of a parallelization chip composed of at least four layers: cap layer, oil and water distribution networks and drop generation layer(s). (B) A close-up illustration image of the flow-focusing DGU in the generation layer. (C) A single corner or petal that can be treated as an independent unit, DGUs in a petal share inlet and outlet. (with kind permission of Royal Society of Chemistry[339])

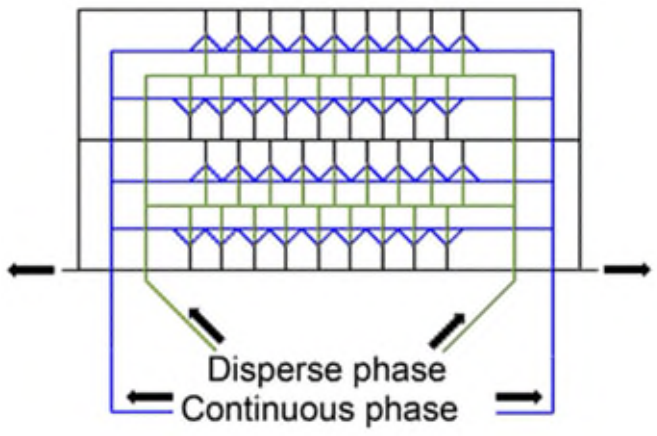

Figure 48. Ladder-type network of cross junctions integrated into a single chip. Three microfluidic layers stacked on top of each other (redrawn with kind permission of American Chemical Society [340])

Nisisako and Torii successfully incorporated a 42 x 42 mm chip with 256 DGUs consisting of 128 inlet holes for the disperse phase and 64 inlet holes for the continuous phase for the preparation of photopolymerizable acrylate monomer droplets (Figure 49).[341] The key feature of this design was the bifurcation geometry which allowed the reduction of the number of inlet holes and the device size.

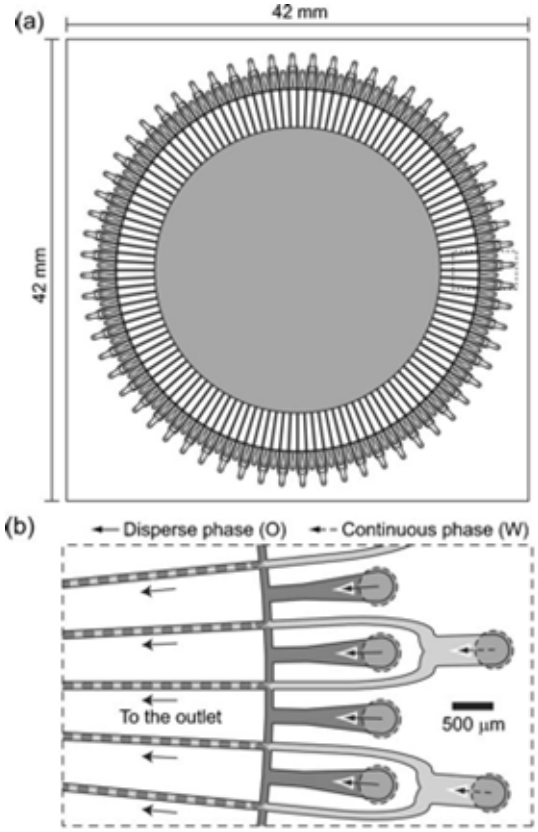

Figure 49. Planar microfluidic geometries for mass-producing monodisperse droplets. (a) Schematic of the 128 cross-junctions on a chip. (b) Schematic of the magnified view of the cross junctions with flow configurations (with kind permission of the Royal Society of Chemistry[341])

6.2. Multiple droplets formation

Romanowsky et al. developed microfluidic devices that integrated up to 15 DGUs in either a 2-D or 3-D array for producing double emulsions with high uniformity and high throughput.[86] These devices could produce single-core double emulsion at rates over 1 kg day^{-1} with a droplet diameter variation of less than 6%. The design provided an efficient route to increase the throughput even though it followed a relatively simple scaling strategy. Figure 49 illustrates the schematic sketches of the DGUs in 0-, 1-, 2- and 3 dimensions. The basic one-step double emulsion generation unit (Figure 18b, 50a) was repeated and connected using a network of larger distribution and collection channels in both a 2-D and 3-D array. The DGUs were connected using a single set of distribution and collection channels (Figure 50b). The 2-D arrays were formed by connecting all layers of DGUs to larger inlets and outlets (Figure 50c). Finally, 2-D arrays were stacked on each other to form a 3-D array (Figure 50d). To produce similar-sized droplets, the distribution channels were designed with lower flow resistance than the DGU to ensure an even distribution of the input fluids to all DGUs. Furthermore, the failure of one DGU would not affect the performance of the others.

Another strategy to increase the throughput during double emulsion formation is to use splitting arrays. This design includes a series of channels that are split into two channels several times and such positions are denoted as “forks”. As a drop encounters a fork, it can choose to cross through one path or split into two smaller drops at each path. This process depends on the flow properties, channel dimensions, and interfacial tension of the fluids. Abate and Weitz implemented a splitting array at the end of the channel to split core/shell droplets into smaller droplets as shown in Figure 51.[342] The parent droplet was split consecutively 3 times to produce 8 similar daughter droplets.

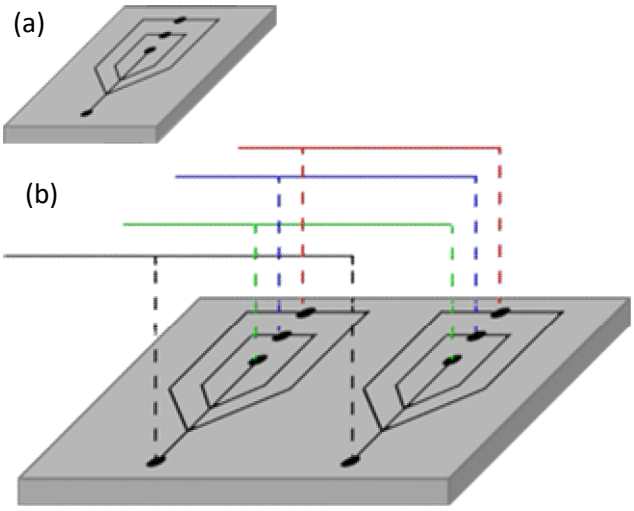

Figure 50. Double emulsification chips can comprise (from (a) to (d)) 0-, 1-, 2-, and 3-dimensional tilings of microfluidic drop maker units (redrawn with kind permission of the Royal Society of Chemistry[86])

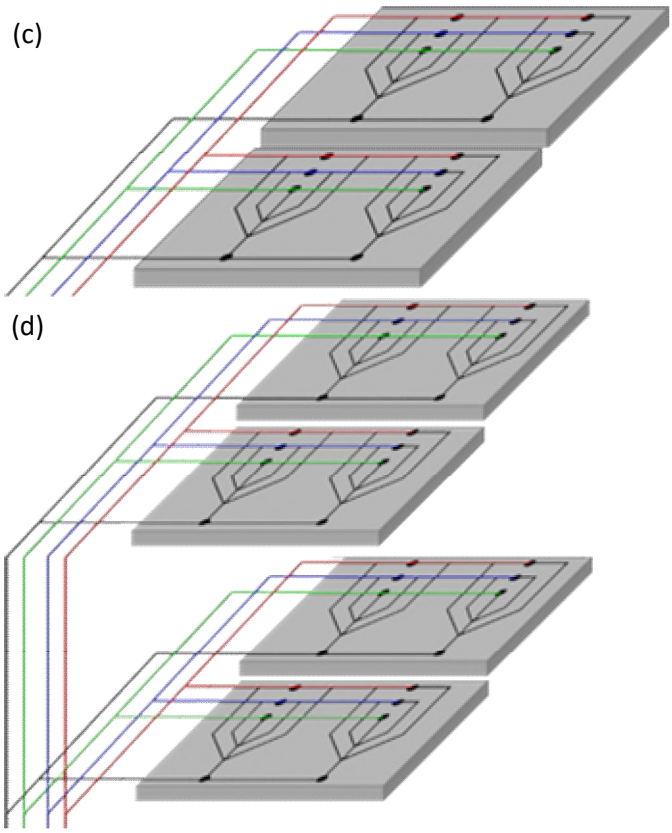

Figure 50. (continued).

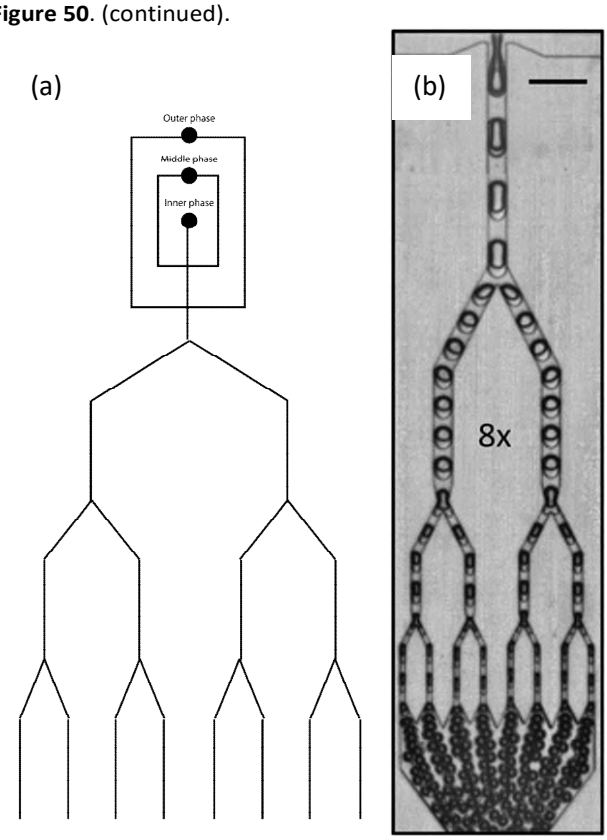

Figure 51. (a) A 3-level tree-type layout splitting array for production of double emulsions; (b) microscope image of core/shell droplets formed by splitting original core/shell droplets into 8 equal portions (with kind permission of the Royal Society of Chemistry[342])

6.3. Scale-up strategies calculation

Admittedly, reaching flow rates and product throughputs by manufacturing in tiny devices sounds like a paradox, but nature teaches us every day how innumerable cells can produce mega-scale outputs. Following this idea of "equalling up" of production, the concepts of external numbering up and internal numbering up were introduced and coined as basic concepts, which are still widely used in the microreactor community.[343] The external numbering up relies on the parallel action of complete microdevices and is effective typically on a level of up to a very few 10 microdevices; with severe limits to be higher alone for cost reasons. Companies like Hitachi have used external numbering-up for piloting chemical production.[344] The internal numbering is more cost-efficient as it uses the relatively chip elemental microstructures, being foils, platelets, etc. They can be stacked at numbers of hundreds if needed. In this way, we have shown the first micromixer operating at an industrial lower bulk scale of 3.5 tons per litre.[345] This internal parallelisation concept follows the famous example of making microdroplets in the bubble and inkjet printers, invented by Siemens, Epson, Hewlett-Packard, and Canon, in the 70s and 80s.[346] Thousands of microholes are operated in parallel, and even with different colors (different solutions). Also, Weitz et al. have shown the fast formation of myriads of droplets via reaching impressive numbering-up levels in microchips with a large number of more than 500 nozzles on a single chip that produces up to 150 ml/h of highly monodisperse drops.[347] Pfizer's Vaccine Manufacturing utilises an external numbering-up of 100 static mixers, using impingement jet microfluidics, to increase the vaccine productivity at their site in Kalamazoo (US) to 100 million doses/month.[348]

We have demonstrated this concept for multiphase flows at a numbering-up level of 8 in a robust, well-engineered microreactor meant for industrial applications at a kilo-lab flow rate, and design criteria and methodology were given.[349-351] For any higher flow rates, flow reactors of higher internal dimensions may be utilised, as Corning's Advanced Flow Reactors.[352, 353] Those reactors operate at milli dimensions but are almost as effective as their micro-scale counterparts by effectively inducing micro-scale convection patterns, which can result in the formation of microdroplets. Hundreds of such flow reactors are currently in global industrial use for production, which demonstrates their ability to fulfil commercial specs. Other commercial microreactor manufacturers as Ehrfeld Mikrotechnik offer similar 'microdevices' aiming at large scales. Their MIPROWA production reactor for Shaoxing Eastlake Biochemical (China) was designed for a production capacity of up to 10,000 t/a. A throughput of about 1000 l/h has a width of 400 mm and a length of 7 m and contains about 150 rectangular reaction channels with exchangeable static mixers.[354, 355]

Assuming that a single microchannel may be operated at a flow rate of up to 1 l/h,[356] and that internal numbering up in the style of Weitz et al. can reach a parallelisation degree of several hundred channels and more (we assume here 1000 for simplicity), a throughput of 1 t/h is not out of reach. 1 t/h would

translate to about 8500 t/a for continuously uninterrupted operation. The specialty fertilisers targeted here are not made millions t/a scale as typical nitrate or ammonia-based fertilisers. The "specialty-chemical scale" of a few 10,000 t/a is most appropriate and can be reached by external numbering up of 5-10 microreactor blocks of above said the very high degree of internal parallelisation.

Conclusions

Traditional fertilisers have a large impact on the environment through over-fertilization and nutrient leaching. Therefore, the development of smart fertilisers that enable precise delivery of nutrients with controlled release kinetics is critically important and successful designs of nanofertiliser have the potential to have a significant impact in the agriculture sector. Nevertheless, high production costs and a lack of knowledge of release behaviour and plant's nutrient uptake has slowed the development and implementation of nanofertilisers. These challenges may be overcome by using microfluidic devices to produce nanofertilisers with well-defined compositions, structures, and functionalities. For example, it may allow the design of materials with specific characteristics, such as heat resistance, chemical durability, pH responsiveness, biodegradability, controlled release, and triggered release. Formulations produced by microfluidic devices have been successfully implemented in some industries, most notably for the production of pharmaceuticals, which demonstrates the potential of this technology. The main hurdle to the widespread application of microfluidics to produce nanofertilizers is it is relatively low throughout. Consequently, further research is required to develop effective scale-up strategies. Alternatively, microfluidic devices can be used to produce nanofertilizers with well-defined properties (compositions, dimensions, and structures), which can then be tested for their efficacy. The well-defined characteristics of these formulations would facilitate the identification of the most critical features contributing to their functionality. This knowledge could then be used to create more effective nanopesticide formulations using conventional methods.

Author Contributions

We strongly encourage authors to include author contributions and recommend using CRediT for standardised contribution descriptions. Please refer to our general author guidelines for more information about authorship.

Conflicts of interest

There are no conflicts to declare.

Acknowledgements

Volker Hessel and Nam Nghiep Tran acknowledge support from the ERC Grant Surface-COnfined fast modulated Plasma for process and Energy intensification (SCOPE) from the European Commission with Grant No. 810182.

References

1. FAO, *Journal*, 2009, 1-7.
2. W. H. Organization, 2014.
3. S. B. S. Clair and J. P. Lynch, *Plant and Soil*, 2010, **335**, 101-115.
4. X. Zhang, E. A. Davidson, D. L. Mauzerall, T. D. Searchinger, P. Dumas and Y. Shen, *Nature*, 2015, **528**, 51-59.
5. X. Cirera and E. Masset, *Philosophical Transactions of the Royal Society B: Biological Sciences*, 2010, **365**, 2821-2834.
6. R. V. Rojas, M. Achouri, J. Maroulis and L. Caon, *Environmental Earth Sciences*, 2016, **75**, 180.
7. T. Gomiero, *Sustainability*, 2016, **8**, 281.
8. H. Blanco-Canqui and R. Lal, in *Principles of Soil Conservation and Management*, Springer, 2010, pp. 493-512.
9. D. Chalise, L. Kumar and P. Kristiansen, *Soil Systems*, 2019, **3**, 12.
10. L. Tadesse, K. Suryabhagavan, G. Sridhar and G. Legesse, *International soil and water conservation research*, 2017, **5**, 85-94.
11. D. Wuepper, P. Borrelli and R. Finger, *Nature Sustainability*, 2020, **3**, 51-55.
12. F.-J. Zhao, Y. Ma, Y.-G. Zhu, Z. Tang and S. P. McGrath, *Environmental science & technology*, 2015, **49**, 750-759.
13. F. Carré, J. Caudeville, R. Bonnard, V. Bert, P. Boucard and M. Ramel, in *Global Soil Security*, Springer, 2017, pp. 275-295.
14. C. Özkul, *Environmental monitoring and assessment*, 2016, **188**, 284.
15. H. Liu, A. Probst and B. Liao, *Science of the total environment*, 2005, **339**, 153-166.
16. J. Bech, *Environmental geochemistry and health*, 2020, 1-6.
17. P. Rengasamy, in *Oxford Research Encyclopedia of Environmental Science*, 2016.
18. R. M. A. Machado and R. P. Serralheiro, *Horticulturae*, 2017, **3**, 30.
19. Z. Wang, B. Fan and L. Guo, *European Journal of Soil Science*, 2019, **70**, 20-24.
20. F. Zulfiqar, M. Navarro, M. Ashraf, N. A. Akram and S. Munné-Bosch, *Plant Science*, 2019, **289**, 110270.
21. Y. Zheng, X. Chen, W. Lin, Z. Cao, X. Zhu, B. Zeng and M. Xu, 2018.
22. R. Liu and R. Lal, *Science of the total environment*, 2015, **514**, 131-139.
23. A. A. Feregrino-Perez, E. Magaña-López, C. Guzmán and K. Esquivel, *Scientia Horticulturae*, 2018, **238**, 126-137.
24. P. Solanki, A. Bhargava, H. Chhipa, N. Jain and J. Panwar, in *Nanotechnologies in food and agriculture*, Springer, 2015, pp. 81-101.
25. K. Congreves and L. Van Eerd, *Nutrient cycling in agroecosystems*, 2015, **102**, 299-318.
26. N. Zuverza-Mena, D. Martínez-Fernández, W. Du, J. A. Hernandez-Viezcas, N. Bonilla-Bird, M. L. López-Moreno, M. Komárek, J. R. Peralta-Videa and J. L. Gardea-Torresdey, *Plant Physiology and Biochemistry*, 2017, **110**, 236-264.
27. H. Bley, C. Gianello, L. d. S. Santos and L. P. R. Selau, *Revista Brasileira de Ciência do Solo*, 2017, **41**.
28. J. Chen and X. Wei, *Nitrogen in Agriculture-Updates*, 2018.
29. N. Kottegoda, I. Munaweera, N. Madusanka and V. Karunaratne, *Current science*, 2011, 73-78.
30. S. Kundu, A. Tapan, M. Vassanda Coumar, S. Rajendiran and S. Mohanty, *Reduction in nitrous oxide emission from nano zinc oxide and nano rock phosphate coated urea*, 2016, 59-70.
31. N. Kottegoda, C. Sandaruwan, G. Priyadarshana, A. Siriwardhana, U. A. Rathnayake, D. M. Berugoda Arachchige, A. R. Kumarasinghe, D. Dahanayake, V. Karunaratne and G. A. Amaratunga, *ACS nano*, 2017, **11**, 1214-1221.
32. H. M. A. Aziz, M. N. Hasaneen and A. M. Omer, *Spanish Journal of Agricultural Research*, 2016, **14**, 17.

33. E. I. Pereira, C. C. da Cruz, A. Solomon, A. Le, M. A. Cavigelli and C. Ribeiro, *Industrial & Engineering Chemistry Research*, 2015, **54**, 3717-3725.
34. R. Liu and R. Lal, *Scientific reports*, 2014, **4**, 1-6.
35. P. Yugandhar and N. Savithramma, *Int J Adv Res*, 2013, **1**, 89-103.
36. M. Delfani, M. Baradarn Firouzabadi, N. Farrokhi and H. Makarian, *Communications in soil science and plant analysis*, 2014, **45**, 530-540.
37. S. León-Silva, R. Arrieta-Cortes, F. Fernández-Luqueño and F. López-Valdez, in *Agricultural Nanobiotechnology*, Springer, 2018, pp. 17-31.
38. M. C. Kyriacou and Y. Rouphael, *Scientia Horticulturae*, 2018, **234**, 463-469.
39. E. Mastronardi, P. Tsae, X. Zhang, C. Monreal and M. C. DeRosa, in *Nanotechnologies in food and agriculture*, Springer, 2015, pp. 25-67.
40. A. Manik and K. Subramanian, *African Journal of Agricultural Research*, 2014, **9**, 276-284.
41. J. Hu, H. Guo, J. Li, Q. Gan, Y. Wang and B. Xing, *Environmental pollution*, 2017, **221**, 199-208.
42. M. Yuvaraj and K. Subramanian, *Journal of plant nutrition*, 2018, **41**, 311-320.
43. A. Lateef, R. Nazir, N. Jamil, S. Alam, R. Shah, M. N. Khan and M. Saleem, *Microporous and Mesoporous Materials*, 2016, **232**, 174-183.
44. T. Jamnongkan and S. Kaewpirom, *Sci J UBU*, 2010, **1**, 43-50.
45. X. Li, Q. Li, X. Xu, Y. Su, Q. Yue and B. Gao, *Journal of the Taiwan Institute of Chemical Engineers*, 2016, **60**, 564-572.
46. T. Jamnongkan and S. Kaewpirom, *Journal of Polymers and the Environment*, 2010, **18**, 413-421.
47. N. E. Rabat, S. Hashim and R. A. Majid, *Procedia engineering*, 2016, **148**, 201-207.
48. M. Zhang, B. Gao, J. Chen, Y. Li, A. E. Creamer and H. Chen, *Chemical Engineering Journal*, 2014, **255**, 107-113.
49. Q. Liu, B. Chen, Q. Wang, X. Shi, Z. Xiao, J. Lin and X. Fang, *Nano letters*, 2009, **9**, 1007-1010.
50. K. Lubkowski, *Environmental Engineering & Management Journal (EEMJ)*, 2014, **13**.
51. C. V. Subbarao, G. Kartheek and D. Sirisha, *International Journal of Applied science and engineering*, 2013, **11**, 25-30.
52. C. Adams, J. Frantz and B. Bugbee, *Journal of plant nutrition and soil science*, 2013, **176**, 76-88.
53. M. Y. Naz and S. A. Sulaiman, *Journal of Controlled Release*, 2016, **225**, 109-120.
54. P. Ashkavand, M. Zarafshar, M. Tabari, J. Mirzaie, A. Nikpour, S. K. Bordbar, D. Struve and G. G. Striker, *Boletín de la Sociedad Argentina de Botánica*, 2018, **53**, 207-219.
55. M. Calabi-Floody, J. Medina, C. Rumpel, L. M. Condron, M. Hernandez, M. Dumont and M. de la Luz Mora, in *Advances in agronomy*, Elsevier, 2018, vol. 147, pp. 119-157.
56. V. Hessel and H. Löwe, *Chemical Engineering Technology: Industrial Chemistry-Plant Equipment-Process Engineering-Biotechnology*, 2003, **26**, 391-408.
57. W. Ehrfeld, V. Hessel, H. Möbius, T. Richter and K. Russow, *DECHEMA MONOGRAPHIEN*, 1995, 1-28.
58. S.-H. Kim, J. W. Kim, J.-C. Cho and D. A. Weitz, *Lab on a Chip*, 2011, **11**, 3162-3166.
59. Z. Liu, F. Fontana, A. Python, J. T. Hirvonen and H. A. Santos, *Small*, 2020, **16**, 1904673.
60. Y.-C. Tan, S.-Y. Teh and A. P. Lee, in *Springer Handbook of Nanotechnology*, Springer, 2010, pp. 553-569.
61. M. G. Bah, H. M. Bilal and J. Wang, *Soft Matter*, 2020, **16**, 570-590.
62. S. T. Sanjay, W. Zhou, M. Dou, H. Tavakoli, L. Ma, F. Xu and X. Li, *Advanced drug delivery reviews*, 2018, **128**, 3-28.
63. D. Liu, H. Zhang, F. Fontana, J. T. Hirvonen and H. A. Santos, *Advanced drug delivery reviews*, 2018, **128**, 54-83.
64. J. Ahn, J. Ko, S. Lee, J. Yu, Y. Kim and N. L. Jeon, *Advanced drug delivery reviews*, 2018, **128**, 29-53.
65. S. Colombo, M. Beck-Broichsitter, J. P. Bøtker, M. Malmsten, J. Rantanen and A. Bohr, *Advanced drug delivery reviews*, 2018, **128**, 115-131.
66. G. Luo, L. Du, Y. Wang and K. Wang, *Chemical Engineering & Technology*, 2019, **42**, 1996-2008.
67. E. Swider, O. Koshkina, J. Tel, L. J. Cruz, I. J. M. de Vries and M. Srinivas, *Acta biomaterialia*, 2018, **73**, 38-51.
68. S. Y. Kashani, A. Afzalian, F. Shirinichi and M. K. Moraveji, *RSC Advances*, 2021, **11**, 229-249.
69. F. M. Galogahi, Y. Zhu, H. An and N.-T. Nguyen, *Journal of Science: Advanced Materials and Devices*, 2020.
70. Q. H. Pho, D. Losic, K. K. Ostrikov, N. N. Tran and V. Hessel, *Reaction Chemistry Engineering*, 2020, **5**, 1374-1396.
71. I. O. Adisa, V. L. R. Pullagurala, J. R. Peralta-Videa, C. O. Dimkpa, W. H. Elmer, J. L. Gardea-Torresdey and J. C. White, *Environmental Science: Nano*, 2019, **6**, 2002-2030.
72. L. Marchiol, M. Iafisco, G. Fellet and A. Adamiano, in *Advances in Agronomy*, Elsevier, 2020, vol. 161, pp. 27-116.
73. G. Muschiolik, *Current Opinion in Colloid & Interface Science*, 2007, **12**, 213-220.
74. E.-M. Varka, E. Tsatsaroni, N. Xristoforidou and A.-M. Darda, *Open Journal of Applied Sciences*, 2012, **2**, 139.
75. W. Wang, M.-J. Zhang and L.-Y. Chu, *Current opinion in pharmacology*, 2014, **18**, 35-41.
76. M. Kakran and M. N. Antipina, *Current Opinion in Pharmacology*, 2014, **18**, 47-55.
77. G. M. Whitesides, *Nature*, 2006, **442**, 368-373.
78. T. Nisisako, S. Okushima and T. Torii, *Soft Matter*, 2005, **1**, 23-27.
79. J. Atencia and D. J. Beebe, *Nature*, 2005, **437**, 648-655.
80. C. O. Dimkpa and P. S. Bindraban, *Journal of agricultural and food chemistry*, 2017, **66**, 6462-6473.
81. L. Y. Chu, A. S. Utada, R. K. Shah, J. W. Kim and D. A. Weitz, *Angewandte Chemie*, 2007, **119**, 9128-9132.
82. G. Vladisavljević, I. Kobayashi and M. Nakajima, *Microfluidics and nanofluidics*, 2012, **13**, 151-178.
83. M. Zhang, W. Wang, R. Xie, X. Ju, Z. Liu, L. Jiang, Q. Chen and L. Chu, *Particuology*, 2016, **24**, 18-31.
84. R. K. Shah, J.-W. Kim, J. J. Agresti, D. A. Weitz and L.-Y. Chu, *Soft Matter*, 2008, **4**, 2303-2309.
85. K.-Y. Lien, S.-H. Lee, T.-J. Tsai, T.-Y. Chen and G.-B. Lee, *Microfluidics and nanofluidics*, 2009, **7**, 795.
86. M. B. Romanowsky, A. R. Abate, A. Rotem, C. Holtze and D. A. Weitz, *Lab on a Chip*, 2012, **12**, 802-807.
87. B. Singh, *Journal of Eco-friendly Agriculture*, 2019, **14**, 43-54.
88. D. An, L. Yang, B. Liu, T.-J. Wang and C. Kan, *Journal of agricultural and food chemistry*, 2017, **65**, 10868-10874.
89. G. M. Blouin, D. W. Rindt and O. E. Moore, *Journal of Agricultural and Food Chemistry*, 1971, **19**, 801-808.
90. F. E. Babadi, R. Yunus, S. A. Rashid, M. A. M. Salleh and S. Ali, *Particuology*, 2015, **23**, 62-67.
91. T. El Assimi, O. Lakbita, A. El Meziane, M. Khouloud, A. Dahchour, R. Beniazza, R. Boulif, M. Raihane and M. Lahcini, *International Journal of Biological Macromolecules*, 2020.
92. A. Kalia, S. P. Sharma, H. Kaur and H. Kaur, in *Multifunctional Hybrid Nanomaterials for Sustainable Agri-Food and Ecosystems*, Elsevier, 2020, pp. 99-134.
93. S. I. Sempeho, H. T. Kim, E. Mubofu and A. Hilonga, 2014.
94. M. Naz, S. Sulaiman, B. Ariwahjoedi and K. Shaari, *Surface Engineering*, 2015, **31**, 486-491.
95. M. Devassine, F. Henry, P. Guerin and X. Briand, *International Journal of Pharmaceutics*, 2002, **242**, 399-404.
96. Y. YU, H.-t. ZOU, J. WANG, M. Xu, Y. LIU and Y.-l. ZHANG, *Plant Nutrition and Fertilizer Science*, 2012, **5**.
97. H. Zou, Y. Ling, Y. Yu, Y. Zhang and N. Yu, *Guang pu xue yu Guang pu fen xi= Guang pu*, 2015, **35**, 3262-3267.
98. Z. Zhou, C. Du, Y. Shen and J.-m. ZHOU, *Journal of Functional Materials*, 2013, **9**.
99. Z. Zhou, C. Du, T. Li, Y. Shen, Y. Zeng, J. Du and J. Zhou, *Environmental Science and Pollution Research*, 2015, **22**, 8672-8682.
100. S. Chen, M. Yang, C. Ba, S. Yu, Y. Jiang, H. Zou and Y. Zhang, *Science of The Total Environment*, 2018, **615**, 431-437.
101. S. Akmaz, E. Dilaver Adıgüzel, M. Yasar and O. Erguven, *Advances in Materials Science and Engineering*, 2013, **2013**.
102. Y. Kusumastuti, M. Kobayashi, F. Y. Purwaningtyas, M. Najmina, H. T. B. M. Petrus, N. R. EVIANA, B. PUTRI and M. Tanihara, *Journal of Engineering Science and Technology*, 2018, **13**, 3500-3506.

103. Z. Dawn, C. V. Liew and P. W. Heng, *International journal of pharmaceutics*, 2009, **377**, 16-24.
104. L. F. Brown and H. S. Fogler, *Professional Reference Shelf, University of Michigan*, 2008.
105. N. Firuzian, R. Sotudeh-Gharebagh and N. Mostoufi, *Particuology*, 2014, **16**, 69-74.
106. C. Goniva, C. Kloss, N. G. Deen, J. A. Kuipers and S. Pirker, *Particuology*, 2012, **10**, 582-591.
107. P. D. Hede, P. Bach and A. D. Jensen, *Industrial & engineering chemistry research*, 2009, **48**, 1893-1904.
108. K. A. Ibrahim, M. Y. Naz, S. Shukrullah, S. A. Sulaiman, A. Ghaffar and N. AbdEl-Salam, *BioResources*, 2019, **14**, 7775-7789.
109. S. Jin, G. Yue, L. Feng, Y. Han, X. Yu and Z. Zhang, *Journal of agricultural and food chemistry*, 2011, **59**, 322-327.
110. R. Liang and M. Liu, *Journal of agricultural and food chemistry*, 2006, **54**, 1392-1398.
111. B. S. Fernandes, J. C. Pinto, E. C. d. M. Cabral-Albuquerque and R. L. L. Fialho, *Polímeros*, 2019, **29**.
112. W. Iley, *Powder technology*, 1991, **65**, 441-445.
113. L. Liu and J. Litster, *Powder Technology*, 1993, **74**, 215-230.
114. M. Tzika, S. Alexandridou and C. Kiparissides, *Powder technology*, 2003, **132**, 16-24.
115. I. M. Bamatov, E. V. Rumyantsev and D. M. Bamatov, 2019.
116. I. M. Bamatov, E. V. Rumyantsev and D. M. Bamatov, 2019.
117. H. Guo, J. C. White, Z. Wang and B. Xing, *Current Opinion in Environmental Science & Health*, 2018, **6**, 77-83.
118. D. Tilman, K. G. Cassman, P. A. Matson, R. Naylor and S. Polasky, *Nature*, 2002, **418**, 671-677.
119. J. Hayles, L. Johnson, C. Worthley and D. Losic, in *New pesticides and soil sensors*, Elsevier, 2017, pp. 193-225.
120. H. M. C. de Azeredo, L. H. C. Mattoso and T. H. McHugh, *Advances in diverse industrial applications of nanocomposites*, 2011, 57-78.
121. E. I. Pereira, F. B. Minussi, C. C. da Cruz, A. C. Bernardi and C. Ribeiro, *Journal of agricultural and food chemistry*, 2012, **60**, 5267-5272.
122. B. Roshanravan, S. Mahmoud Soltani, F. Mahdavi, S. Abdul Rashid and M. Khanif Yusop, *Chemical Speciation & Bioavailability*, 2014, **26**, 249-256.
123. B. Roshanravan, S. M. Soltani, S. A. Rashid, F. Mahdavi and M. K. Yusop, *Chemical Speciation & Bioavailability*, 2015, **27**, 44-51.
124. X. He and H.-M. Hwang, *journal of food and drug analysis*, 2016, **24**, 671-681.
125. R. Suresh, S. Borkar, V. Sawant, V. Shende and S. Dimble, *International Journal of Pharmaceutical Sciences and Nanotechnology*, 2010, **3**, 901-905.
126. M. Everaert, R. Warrinnier, S. Baken, J.-P. Gustafsson, D. De Vos and E. Smolders, *ACS Sustainable Chemistry & Engineering*, 2016, **4**, 4280-4287.
127. P. Songkhum, T. Wuttikhun, N. Chanlek, P. Khemthong and K. Laohhasurayotin, *Applied Clay Science*, 2018, **152**, 311-322.
128. N. Kottegoda, C. Sandaruwan, P. Perera, N. Madusanka and V. Karunaratne, *Nanoscience & Nanotechnology-Asia*, 2014, **4**, 94-102.
129. N. Kottegoda, N. Madusanka and C. Sandaruwan, *Indian J Agr Sci*, 2016, **86**, 494-499.
130. H. Wanyika, E. Gatebe, P. Kioni, Z. Tang and Y. Gao, *Journal of nanoscience and nanotechnology*, 2012, **12**, 2221-2228.
131. K.-Z. Hossain, C. M. Monreal and A. Sayari, *Colloids and Surfaces B: Biointerfaces*, 2008, **62**, 42-50.
132. A. Mukherjee, S. Majumdar, A. D. Servin, L. Pagano, O. P. Dhankher and J. C. White, *Frontiers in plant science*, 2016, **7**, 172.
133. P. L. Kashyap, X. Xiang and P. Heiden, *International journal of biological macromolecules*, 2015, **77**, 36-51.
134. E. Corradini, M. De Moura and L. Mattoso, *Express Polymer Letters*, 2010, **4**.
135. M. Yuvaraj and K. Subramanian, *Soil science and plant nutrition*, 2015, **61**, 319-326.
136. W. Pang, D. Hou, H. Wang, S. Sai, B. Wang, J. Ke, G. Wu, Q. Li and M. T. Holtzapple, *Journal of the Brazilian Chemical Society*, 2018, **29**, 2397-2404.
137. C. P. Champagne and P. Fustier, *Current opinion in biotechnology*, 2007, **18**, 184-190.
138. Y. Zhang, L. Li, F. Tang and J. Ren, *Journal of nanoscience and nanotechnology*, 2006, **6**, 3210-3214.
139. J. Song, F. Babayekhorasani and P. T. Spicer, *Biomacromolecules*, 2019, **20**, 4437-4446.
140. L. Mei, F. He, R.-Q. Zhou, C.-D. Wu, R. Liang, R. Xie, X.-J. Ju, W. Wang and L.-Y. Chu, *ACS Applied Materials & Interfaces*, 2014, **6**, 5962-5970.
141. J. Xu, X. Xu, H. Zhao and G. Luo, *Sensors and Actuators B: Chemical*, 2013, **183**, 201-210.
142. B. M. A. N. Estevinho, F. A. N. Rocha, L. M. D. S. Santos and M. A. C. Alves, *Journal of microencapsulation*, 2013, **30**, 571-579.
143. Y. Bashan, *Applied and environmental microbiology*, 1986, **51**, 1089-1098.
144. Y. Yang, M. Zhang, Y. Li, X. Fan and Y. Geng, *Soil Science Society of America Journal*, 2012, **76**, 2307-2317.
145. D. França, Â. F. Medina, L. L. Messa, C. F. Souza and R. Faez, *Carbohydrate polymers*, 2018, **196**, 47-55.
146. M. M. Rahman, J. Tsukamoto, Y. Tokumoto and M. A. R. Shuvo, *J For Sci*, 2013, **29**, 38-48.
147. J. Behin and N. Sadeghi, *International Journal of Recycling of Organic Waste in Agriculture*, 2016, **5**, 289-299.
148. G.-J. Jiao, Q. Xu, S.-L. Cao, P. Peng and D. She, *BioResources*, 2018, **13**, 1711-1728.
149. T. S. Pierre and E. Chiellini, *Journal of bioactive and compatible polymers*, 1986, **1**, 467-497.
150. T. St Pierre and E. Chiellini, *Journal of bioactive and compatible polymers*, 1987, **2**, 4-30.
151. R. Cameron and A. Kamvari-Moghaddam, *Journal*, 2008.
152. A. Göpferich, *Biomaterials*, 1996, **17**, 103-114.
153. C. Bastioli, *Handbook of biodegradable polymers*, Walter de Gruyter GmbH & Co KG, 2020.
154. M. R. Hussain, R. R. Devi and T. K. Maji, *Iranian Polymer Journal*, 2012, **21**, 473-479.
155. R. C. Sabadini, V. C. Martins and A. Pawlicka, *Cellulose*, 2015, **22**, 2045-2054.
156. S. Noppakundilograt, N. Pheatcharat and S. Kiatkamjornwong, *Journal of Applied Polymer Science*, 2015, **132**.
157. N. Ahmad, W. Fernando and M. Uzir, *Biosystems Engineering*, 2015, **129**, 78-86.
158. B. R. dos Santos, F. B. Bacalhau, T. dos Santos Pereira, C. F. Souza and R. Faez, *Carbohydrate polymers*, 2015, **127**, 340-346.
159. R. Celis, M. Adelino, M. Hermosín and J. Cornejo, *Journal of hazardous materials*, 2012, **209**, 67-76.
160. E. I. Pereira, A. S. Giroto, A. Bortolin, C. F. Yamamoto, J. M. Marconcini, A. C. de Campos Bernardi and C. Ribeiro, *Nanotechnologies in food and agriculture*, 2015, 241-265.
161. A. M. Senna, J. B. do Carmo, J. M. S. da Silva and V. R. Botaro, *Journal of Environmental Chemical Engineering*, 2015, **3**, 996-1002.
162. M. M. Costa, E. C. Cabral-Albuquerque, T. L. Alves, J. C. Pinto and R. L. Fialho, *Journal of agricultural and food chemistry*, 2013, **61**, 9984-9991.
163. A. Roy, S. K. Singh, J. Bajpai and A. K. Bajpai, *Central European Journal of Chemistry*, 2014, **12**, 453-469.
164. R. Grillo, Z. Clemente, J. L. de Oliveira, E. V. R. Campos, V. C. Chalupe, C. M. Jonsson, R. de Lima, G. Sanches, C. S. Nishisaka and A. H. Rosa, *Journal of hazardous materials*, 2015, **286**, 562-572.
165. K. Lubkowski and B. Grzmil, *Polish Journal of Chemical Technology*, 2007, **9**, 81-84.
166. M. A. Melaj and M. E. Daraio, *Journal of Applied Polymer Science*, 2014, **131**.
167. B. Azeem, K. KuShaari, Z. B. Man, A. Basit and T. H. Thanh, *Journal of Controlled Release*, 2014, **181**, 11-21.
168. T. Kawakatsu, Y. Kikuchi and M. Nakajima, *Journal of the American Oil Chemists' Society*, 1997, **74**, 317-321.
169. Y. Ding, P. D. Howes and A. J. deMello, *Analytical chemistry*, 2019, **92**, 132-149.
170. X. C. i Solvas and A. DeMello, *Chemical Communications*, 2011, **47**, 1936-1942.
171. J.-C. Baret, *Lab on a Chip*, 2012, **12**, 422-433.
172. K. Ren, J. Zhou and H. Wu, *Accounts of chemical research*, 2013, **46**, 2396-2406.

173. M. T. Guo, A. Rotem, J. A. Heyman and D. A. Weitz, *Lab on a Chip*, 2012, **12**, 2146-2155.
174. H. N. Joensson and H. Andersson Svahn, *Angewandte Chemie International Edition*, 2012, **51**, 12176-12192.
175. Y. Ding, J. Choo and A. J. DeMello, *Microfluidics and nanofluidics*, 2017, **21**, 1-20.
176. N. Shembekar, C. Chaipan, R. Utharala and C. A. Merten, *Lab on a Chip*, 2016, **16**, 1314-1331.
177. S. Mashaghi, A. Abbaspourrad, D. A. Weitz and A. M. van Oijen, *TrAC Trends in Analytical Chemistry*, 2016, **82**, 118-125.
178. R. M. Maceiczyk, K. Dümbgen, I. Lignos, L. Protesescu, M. V. Kovalenko and A. J. deMello, *Chemistry of Materials*, 2017, **29**, 8433-8439.
179. A. Suea-Ngam, P. D. Howes, M. Srisa-Art and A. J. DeMello, *Chemical Communications*, 2019, **55**, 9895-9903.
180. L. Cai, J. Marthelot and P.-T. Brun, *Proceedings of the National Academy of Sciences*, 2019, **116**, 22966-22971.
181. T. D. Martz, D. Bardin, P. S. Sheeran, A. P. Lee and P. A. Dayton, *Small*, 2012, **8**, 1876-1879.
182. A. M. Leshansky and L. M. Pismen, *Physics of Fluids*, 2009, **21**, 023303.
183. X. Xu, R. Song, M. He, C. Peng, M. Yu, Y. Hou, H. Qiu, R. Zou and S. Yao, *Lab on a Chip*, 2017, **17**, 3504-3513.
184. J. B. Knight, A. Vishwanath, J. P. Brody and R. H. Austin, *Physical review letters*, 1998, **80**, 3863.
185. I. V. Zhigaltsev, N. Belliveau, I. Hafez, A. K. Leung, J. Huft, C. Hansen and P. R. Cullis, *Langmuir*, 2012, **28**, 3633-3640.
186. A. K. Leung, I. M. Hafez, S. Baoukina, N. M. Belliveau, I. V. Zhigaltsev, E. Afshinmanesh, D. P. Tieleman, C. L. Hansen, M. J. Hope and P. R. Cullis, *The Journal of Physical Chemistry C*, 2012, **116**, 18440-18450.
187. T. A. Balbino, N. T. Aoki, A. A. Gasperini, C. L. Oliveira, A. R. Azzoni, L. P. Cavalcanti and G. Lucimara, *Chemical engineering journal*, 2013, **226**, 423-433.
188. X. Li, N. Anton, T. M. C. Ta, M. Zhao, N. Messaddeq and T. F. Vandamme, *International journal of nanomedicine*, 2011, **6**, 1313.
189. S. Madisetti, Z. Zheng, Z. Gong, S. Penmetsa, Y. Lvov and L. Que, 2009.
190. X.-T. Mu, X.-J. Ju, L. Zhang, X.-B. Huang, Y. Faraj, Z. Liu, W. Wang, R. Xie, Y. Deng and L.-Y. Chu, *Journal of Membrane Science*, 2019, **590**, 117275.
191. C. Kantak, S. Beyer, L. Yobas, T. Bansal and D. Trau, *Lab on a Chip*, 2011, **11**, 1030-1035.
192. J. Pessi, H. A. Santos, I. Miroshnyk, D. A. Weitz and S. Mirza, *International journal of pharmaceutics*, 2014, **472**, 82-87.
193. L. Liu, F. Wu, X.-J. Ju, R. Xie, W. Wang, C. H. Niu and L.-Y. Chu, *Journal of colloid and interface science*, 2013, **404**, 85-90.
194. C.-H. Yeh, Y.-C. Chen and Y.-C. Lin, *Microfluidics and nanofluidics*, 2011, **11**, 245-253.
195. W.-C. Cheng, Y. He, A.-Y. Chang and L. Que, *Biomicrofluidics*, 2013, **7**, 064102.
196. D. Lensen, K. van Breukelen, D. M. Vriezema and J. C. van Hest, *Macromolecular bioscience*, 2010, **10**, 475-480.
197. T. Y. Lee, M. Ku, B. Kim, S. Lee, J. Yang and S. H. Kim, *Small*, 2017, **13**, 1700646.
198. M. F. Thorne, F. Simkovic and A. G. Slater, *Scientific reports*, 2019, **9**, 1-7.
199. N.-D. Dinh, M. Kukumberg, A.-T. Nguyen, H. Keramati, S. Guo, D.-T. Phan, B. Nurdiyana, E. Birgersson, H. L. Leo and R. Y.-J. Huang, *Lab on a Chip*, 2020, **20**, 2756-2764.
200. J. Xu, S. Li, C. Tostado, W. Lan and G. Luo, *Biomedical microdevices*, 2009, **11**, 243-249.
201. K.-S. Huang, T.-H. Lai and Y.-C. Lin, *Lab on a Chip*, 2006, **6**, 954-957.
202. K.-S. Huang, M.-K. Liu, C.-H. Wu, Y.-T. Yen and Y.-C. Lin, *Journal of Micromechanics and Microengineering*, 2007, **17**, 1428.
203. I. U. Khan, C. A. Serra, N. Anton, M. Er-Rafik, C. Blanck, M. Schmutz, I. Kraus, N. Messaddeq, C. Sutter and H. Anton, *International journal of pharmaceutics*, 2015, **493**, 7-15.
204. P. M. Valencia, E. M. Pridgen, M. Rhee, R. Langer, O. C. Farokhzad and R. Karnik, *ACS nano*, 2013, **7**, 10671-10680.
205. L. Zhang, Q. Feng, J. Wang, S. Zhang, B. Ding, Y. Wei, M. Dong, J.-Y. Ryu, T.-Y. Yoon and X. Shi, *ACS nano*, 2015, **9**, 9912-9921.
206. E. Chiesa, A. Greco, F. Riva, E. M. Tosca, R. Dorati, S. Pisani, T. Modena, B. Conti and I. Genta, *International journal of molecular sciences*, 2019, **20**, 6212.
207. Y. Morikawa, T. Tagami, A. Hoshikawa and T. Ozeki, *Biological and Pharmaceutical Bulletin*, 2018, **41**, 899-907.
208. Y. Shin, Y. Lim, T. Kwak, J. H. Hwang, A. Georgescu, D. Huh, D. Kim and T. Kang, *Advanced Functional Materials*, 2021, **31**, 2007856.
209. L. Kong, R. Chen, X. Wang, C.-X. Zhao, Q. Chen, M. Hai, D. Chen, Z. Yang and D. A. Weitz, *Lab on a Chip*, 2019, **19**, 2089-2095.
210. J. Sun, L. Zhang, J. Wang, Q. Feng, D. Liu, Q. Yin, D. Xu, Y. Wei, B. Ding and X. Shi, *Advanced materials*, 2015, **27**, 1402-1407.
211. G. T. Vladisavljević, R. Al Nuumani and S. A. Nabavi, *Micromachines*, 2017, **8**, 75.
212. L. A. Trujillo-Cayado, J. Santos, M. C. Alfaro, N. Calero and J. Muñoz, *Industrial & Engineering Chemistry Research*, 2016, **55**, 7259-7266.
213. J. Santos, L. Trujillo-Cayado, N. Calero, M. Alfaro and J. Muñoz, *Journal of Industrial and Engineering Chemistry*, 2016, **36**, 90-95.
214. A. Abate and D. Weitz, *Small*, 2009, **5**, 2030-2032.
215. T. Nisisako, T. Ando and T. Hatsuzawa, *Small*, 2014, **10**, 5116-5125.
216. J. Huang, W. Li, Y. Li, C. Luo, Y. Zeng, Y. Xu and J. Zhou, *Journal of Materials Chemistry B*, 2014, **2**, 6848-6854.
217. A. D. Stroock, in *Optical Biosensors*, Elsevier, 2008, pp. 659-681.
218. D. Mark, S. Haeberle, G. Roth, F. Von Stetten and R. Zengerle, in *Microfluidics based microsystems*, Springer, 2010, pp. 305-376.
219. N. Hao, Y. Nie and J. X. Zhang, *Biomaterials science*, 2019, **7**, 2218-2240.
220. Y. Song, J. Hormes and C. S. Kumar, *small*, 2008, **4**, 698-711.
221. S. Tanaka, N. Nakatani and Y. Miyake, *Chemistry letters*, 2009, **38**, 780-781.
222. S. Marre and K. F. Jensen, *Chemical Society Reviews*, 2010, **39**, 1183-1202.
223. A. Günther and K. F. Jensen, *Lab on a Chip*, 2006, **6**, 1487-1503.
224. K. F. Jensen, *AIChE Journal*, 2017, **63**, 858-869.
225. D. T. McQuade and P. H. Seeberger, *The Journal of organic chemistry*, 2013, **78**, 6384-6389.
226. N. J. Carroll, S. B. Rathod, E. Derbins, S. Mendez, D. A. Weitz and D. N. Petsev, *Langmuir*, 2008, **24**, 658-661.
227. T. Fu, Y. Ma, D. Funfschilling, C. Zhu and H. Z. Li, *Chemical engineering science*, 2010, **65**, 3739-3748.
228. J. Xu, S. Li, J. Tan, Y. Wang and G. Luo, *AIChE journal*, 2006, **52**, 3005-3010.
229. T. Fu, L. Wei, C. Zhu and Y. Ma, *Chemical Engineering and Processing: Process Intensification*, 2015, **91**, 114-120.
230. M. Y. A. Jamalabadi, M. DaqiqShirazi, A. Kosar and M. S. Shadloo, *Theoretical and Applied Mechanics Letters*, 2017, **7**, 243-251.
231. R. K. Shah, H. C. Shum, A. C. Rowat, D. Lee, J. J. Agresti, A. S. Utada, L.-Y. Chu, J.-W. Kim, A. Fernandez-Nieves and C. J. Martinez, *Materials Today*, 2008, **11**, 18-27.
232. C. Serra, N. Berton, M. Bouquey, L. Prat and G. Hadziioannou, *Langmuir*, 2007, **23**, 7745-7750.
233. A. S. Utada, A. Fernandez-Nieves, H. A. Stone and D. A. Weitz, *Physical review letters*, 2007, **99**, 094502.
234. V. Hessel, H. Löwe and F. Schönfeld, *Chemical Engineering Science*, 2005, **60**, 2479-2501.
235. S. L. Anna, N. Bontoux and H. A. Stone, *Applied physics letters*, 2003, **82**, 364-366.
236. A. S. Utada, E. Lorenceau, D. R. Link, P. D. Kaplan, H. A. Stone and D. Weitz, *Science*, 2005, **308**, 537-541.
237. Z. Chang, C. A. Serra, M. Bouquey, L. Prat and G. Hadziioannou, *Lab on a Chip*, 2009, **9**, 3007-3011.
238. N. Nam-Trung and W. Zhigang, *J Micromech Microeng*, 2005, **15**, R1.
239. F. Bally, C. A. Serra, V. Hessel and G. Hadziioannou, *Chemical Engineering Science*, 2011, **66**, 1449-1462.
240. N. Hao, Y. Nie, Z. Xu, A. B. Closson, T. Usherwood and J. X. Zhang, *Chemical Engineering Journal*, 2019, **366**, 433-438.
241. V. Hessel, H. Löwe and S. Hardt, *Chemical micro process engineering: fundamentals, modelling and reactions*, John Wiley & Sons, 2004.

242. L. Capretto, W. Cheng, M. Hill and X. Zhang, *Microfluidics*, 2011, 27-68.
243. I. Shestopalov, J. D. Tice and R. F. Ismagilov, *Lab on a Chip*, 2004, **4**, 316-321.
244. A. W. Chow, *AIChE Journal*, 2002, **48**, 1590-1595.
245. K. F. Jensen, *Chemical Engineering Science*, 2001, **56**, 293-303.
246. B. P. Mason, K. E. Price, J. L. Steinbacher, A. R. Bogdan and D. T. McQuade, *Chemical reviews*, 2007, **107**, 2300-2318.
247. A. R. Abate, J. Thiele and D. A. Weitz, *Lab on a Chip*, 2011, **11**, 253-258.
248. L. Arriaga, E. Amstad and D. Weitz, *Lab on a Chip*, 2015, **15**, 3335-3340.
249. F. Tu and D. Lee, *Langmuir*, 2012, **28**, 9944-9952.
250. T. Y. Lee, T. M. Choi, T. S. Shim, R. A. Frijns and S.-H. Kim, *Lab on a Chip*, 2016, **16**, 3415-3440.
251. P. B. O'Donnell and J. W. McGinity, *Advanced drug delivery reviews*, 1997, **28**, 25-42.
252. A. Abbaspourrad, N. J. Carroll, S.-H. Kim and D. A. Weitz, *Journal of the American Chemical Society*, 2013, **135**, 7744-7750.
253. N. Pannacci, H. Bruus, D. Bartolo, I. Etchart, T. Lockhart, Y. Hennequin, H. Willaime and P. Tabeling, *Physical review letters*, 2008, **101**, 164502.
254. Z. Nie, S. Xu, M. Seo, P. C. Lewis and E. Kumacheva, *Journal of the American chemical society*, 2005, **127**, 8058-8063.
255. Y. Hennequin, N. Pannacci, C. P. De Torres, G. Tetradis-Meris, S. Chapuliot, E. Bouchaud and P. J. L. Tabeling, 2009, **25**, 7857-7861.
256. J.-O. Nam, J. Kim, S. H. Jin, Y.-M. Chung and C.-S. Lee, *Journal of colloid and interface science*, 2016, **464**, 246-253.
257. S.-H. Kim, J.-G. Park, T. M. Choi, V. N. Manoharan and D. A. Weitz, *Nature Communications*, 2014, **5**, 1-8.
258. P. W. Chen, R. M. Erb and A. R. J. L. Studart, 2012, **28**, 144-152.
259. S.-H. Kim, B. J. J. o. c. Kim and i. science, 2014, **415**, 26-31.
260. T. Kanai, D. Lee, H. C. Shum, R. K. Shah and D. A. J. A. M. Weitz, 2010, **22**, 4998-5002.
261. S. S. Lee, B. Kim, S. K. Kim, J. C. Won, Y. H. Kim and S. H. J. A. M. Kim, 2015, **27**, 627-633.
262. J.-W. Kim, A. Fernández-Nieves, N. Dan, A. S. Utada, M. Marquez and D. A. J. N. L. Weitz, 2007, **7**, 2876-2880.
263. I. U. Khan, L. Stolch, C. A. Serra, N. Anton, R. Akasov and T. F. Vandamme, *International journal of pharmaceutics*, 2015, **478**, 78-87.
264. K. C. Schad and K. Hynynen, *Physics in Medicine & Biology*, 2010, **55**, 4933.
265. N. Reznik, R. Williams and P. N. Burns, *Ultrasound in medicine & biology*, 2011, **37**, 1271-1279.
266. M. L. Fabiilli, K. J. Haworth, N. H. Fakhri, O. D. Kripfgans, P. L. Carson and J. B. Fowlkes, *IEEE transactions on ultrasonics, ferroelectrics, and frequency control*, 2009, **56**, 1006-1017.
267. O. D. Kripfgans, J. B. Fowlkes, D. L. Miller, O. P. Eldevik and P. L. Carson, *Ultrasound in medicine & biology*, 2000, **26**, 1177-1189.
268. R. Williams, C. Wright, E. Cherin, N. Reznik, M. Lee, I. Gorelikov, F. S. Foster, N. Matsuura and P. N. Burns, *Ultrasound in medicine & biology*, 2013, **39**, 475-489.
269. D. Pajek, A. Burgess, Y. Huang and K. Hynynen, *Ultrasound in medicine & biology*, 2014, **40**, 2151-2161.
270. P. S. Sheeran, N. Matsuura, M. A. Borden, R. Williams, T. O. Matsunaga, P. N. Burns and P. A. Dayton, *IEEE transactions on ultrasonics, ferroelectrics, and frequency control*, 2016, **64**, 252-263.
271. F. Malloggi, N. Pannacci, R. Attia, F. Monti, P. Mary, H. Willaime, P. Tabeling, B. Cabane and P. Poncet, *Langmuir*, 2010, **26**, 2369-2373.
272. G. I. Taylor, *Proceedings of the Royal Society of London. Series A, containing papers of a mathematical and physical character*, 1934, **146**, 501-523.
273. L. Shui, A. van den Berg and J. C. T. Eijkel, *Microfluidics and Nanofluidics*, 2011, **11**, 87-92.
274. R. Melich, P. Bussat, L. Morici, A. Vivien, E. Gaud, T. Bettinger and S. Cherkaoui, *International Journal of Pharmaceutics*, 2020, **587**, 119651.
275. A. D. Stroock, S. K. W. Dertinger, A. Ajdari, I. Mezić, H. A. Stone and G. M. Whitesides, *Science*, 2002, **295**, 647-651.
276. N. Hao, Y. Nie and J. X. Zhang, *ACS Sustainable Chemistry & Engineering*, 2018, **6**, 1522-1526.
277. C. J. Brinker, Y. Lu, A. Sellinger and H. Fan, *Advanced materials*, 1999, **11**, 579-585.
278. Z. Hou, C. Zhang, C. Li, Z. Xu, Z. Cheng, G. Li, W. Wang, C. Peng and J. Lin, *Chemistry–A European Journal*, 2010, **16**, 14513-14519.
279. H. Wang, D. Wu, D. Li, Z. Niu, Y. Chen, D. Tang, M. Wu, J. Cao and Y. Huang, *Nanoscale*, 2011, **3**, 3601-3604.
280. J. Wang, C.-K. Tsung, W. Hong, Y. Wu, J. Tang and G. D. Stucky, *Chemistry of materials*, 2004, **16**, 5169-5181.
281. G.-L. Lin, Y.-H. Tsai, H.-P. Lin, C.-Y. Tang and C.-Y. Lin, *Langmuir*, 2007, **23**, 4115-4119.
282. S. Bose and S. K. Saha, *Journal of the American Ceramic Society*, 2003, **86**, 1055-1057.
283. I. Bogdanoviciene, A. Beganskiene, K. Tonsuaadu, J. Glaser, H.-J. Meyer and A. Kareiva, *Materials Research Bulletin*, 2006, **41**, 1754-1762.
284. M. Fathi and A. Hanifi, *Materials letters*, 2007, **61**, 3978-3983.
285. H. Eshtiagh-Hosseini, M. R. Housaindokht and M. Chahkandi, *Materials Chemistry and Physics*, 2007, **106**, 310-316.
286. M. Ashok, S. N. Kalkura, N. M. Sundaram and D. Arivuoli, *Journal of Materials Science: Materials in Medicine*, 2007, **18**, 895-898.
287. H. Bensalah, M. F. Bekheet, S. A. Younssi, M. Ouammou and A. Gurlo, *Journal of environmental chemical engineering*, 2018, **6**, 1347-1352.
288. S. Kuśnieruk, J. Wojnarowicz, A. Chodara, T. Chudoba, S. Gierlotka and W. Lojkowski, *Beilstein journal of nanotechnology*, 2016, **7**, 1586-1601.
289. J. Chen, Z. Wen, S. Zhong, Z. Wang, J. Wu and Q. Zhang, *Materials & Design*, 2015, **87**, 445-449.
290. X. Guo, H. Yan, S. Zhao, Z. Li, Y. Li and X. Liang, *Advanced Powder Technology*, 2013, **24**, 1034-1038.
291. P. M. S. Shanthi, R. Mangalaraja, A. Uthirakumar, S. Velmathi, T. Balasubramanian and M. Ashok, *Journal of colloid and interface science*, 2010, **350**, 39-43.
292. A. Lak, M. Mazloumi, M. S. Mohajerani, S. Zanganeh, M. R. Shayegh, A. Kajbafvala, H. Arami and S. K. Sadrnezhaad, *Journal of the American Ceramic Society*, 2008, **91**, 3580-3584.
293. M. N. Hassan, M. M. Mahmoud, A. Abd El-Fattah and S. Kandil, *Ceramics International*, 2016, **42**, 3725-3744.
294. H. C. Shum, A. Bandyopadhyay, S. Bose and D. A. Weitz, *Chemistry of Materials*, 2009, **21**, 5548-5555.
295. K. Liu and J. Qin, *Nanotechnology*, 2013, **24**, 125602.
296. C. J. Gerdts, V. Tereshko, M. K. Yadav, I. Dementieva, F. Collart, A. Joachimiak, R. C. Stevens, P. Kuhn, A. Kossiakoff and R. F. Ismagilov, *Angewandte Chemie*, 2006, **118**, 8336-8340.
297. R. Rial, R. R. Costa, R. L. Reis, Z. Liu, I. Pashkuleva and J. M. Ruso, *Crystal Growth & Design*, 2019, **19**, 6351-6359.
298. R. Rial, P. G. Tahoces, N. Hassan, M. Cordero, Z. Liu and J. M. Ruso, *Materials Science and Engineering: C*, 2019, **102**, 221-227.
299. D. França, L. L. Messa, C. F. Souza and R. Faez, in *Polymers for Agri-Food Applications*, Springer, 2019, pp. 29-44.
300. D. Pan, X. Liu, M. Liu, Q. Chen, W. Huang and B. Li, *Colloids and Surfaces A: Physicochemical and Engineering Aspects*, 2018, **553**, 652-659.
301. S. S. Tsai, J. S. Wexler, J. Wan and H. A. Stone, *Applied Physics Letters*, 2011, **99**, 153509.
302. B.-U. Moon, N. Hakimi, D. K. Hwang and S. S. Tsai, *Biomicrofluidics*, 2014, **8**, 052103.
303. W. Gao and Y. Chen, *International Journal of Heat and Mass Transfer*, 2019, **135**, 158-163.
304. Z. Z. Chong, S. H. Tan, A. M. Gañán-Calvo, S. B. Tor, N. H. Loh and N.-T. Nguyen, *Lab on a Chip*, 2016, **16**, 35-58.
305. D. R. Link, E. Grasland-Mongrain, A. Duri, F. Sarrazin, Z. Cheng, G. Cristobal, M. Marquez and D. A. Weitz, *Angewandte Chemie International Edition*, 2006, **45**, 2556-2560.
306. S. H. Tan, B. Semin and J.-C. Baret, *Lab on a Chip*, 2014, **14**, 1099-1106.
307. P. Zhu and L. Wang, *Lab on a Chip*, 2017, **17**, 34-75.
308. M. He, J. S. Kuo and D. T. Chiu, *Applied Physics Letters*, 2005, **87**, 031916.
309. P. He, H. Kim, D. Luo, M. Marquez and Z. Cheng, *Applied Physics Letters*, 2010, **96**, 174103.

310. H. Kim, D. Luo, D. Link, D. A. Weitz, M. Marquez and Z. Cheng, *Applied Physics Letters*, 2007, **91**, 133106.
311. S.-H. Tan, N.-T. Nguyen, L. Yobas and T. G. Kang, *Journal of Micromechanics and Microengineering*, 2010, **20**, 045004.
312. C. H. Chen, A. R. Abate, D. Lee, E. M. Terentjev and D. A. Weitz, *Advanced materials*, 2009, **21**, 3201-3204.
313. Y. Wu, T. Fu, Y. Ma and H. Z. Li, *Microfluidics and Nanofluidics*, 2015, **18**, 19-27.
314. E. Surenjav, C. Priest, S. Herminghaus and R. Seemann, *Lab on a Chip*, 2009, **9**, 325-330.
315. C. P. Lee, H. Y. Tsai and M. F. Lai, *Soft Matter*, 2012, **8**, 11537-11543.
316. Y. Wu, T. Fu, Y. Ma and H. Z. Li, *Soft Matter*, 2013, **9**, 9792-9798.
317. J. Liu, S.-H. Tan, Y. F. Yap, M. Y. Ng and N.-T. Nguyen, *Microfluidics and nanofluidics*, 2011, **11**, 177-187.
318. Q. Yan, S. Xuan, X. Ruan, J. Wu and X. Gong, *Microfluidics and Nanofluidics*, 2015, **19**, 1377-1384.
319. S. Kahkeshani and D. Di Carlo, *Lab on a Chip*, 2016, **16**, 2474-2480.
320. C.-P. Lee, T.-S. Lan and M.-F. Lai, *Journal of Applied Physics*, 2014, **115**, 17B527.
321. N.-T. Nguyen, T.-H. Ting, Y.-F. Yap, T.-N. Wong, J. C.-K. Chai, W.-L. Ong, J. Zhou, S.-H. Tan and L. Yobas, *Applied Physics Letters*, 2007, **91**, 084102.
322. S.-H. Tan, S. S. Murshed, N.-T. Nguyen, T. N. Wong and L. Yobas, *Journal of Physics D: Applied Physics*, 2008, **41**, 165501.
323. C. N. Baroud, J.-P. Delville, F. Gallaire and R. Wunenburger, *Physical Review E*, 2007, **75**, 046302.
324. C. A. Stan, S. K. Tang and G. M. Whitesides, *Analytical chemistry*, 2009, **81**, 2399-2402.
325. P. Zhang, H. Bachman, A. Ozcelik and T. J. Huang, *Annual Review of Analytical Chemistry*, 2020, **13**, 17-43.
326. D. J. Collins, Z. Ma and Y. Ai, *Analytical chemistry*, 2016, **88**, 5513-5522.
327. P. Sehgal and B. J. Kirby, *Analytical chemistry*, 2017, **89**, 12192-12200.
328. S. Y. Tang, R. Qiao, Y. Lin, Y. Li, Q. Zhao, D. Yuan, G. Yun, J. Guo, M. D. Dickey and T. J. Huang, *Advanced Materials Technologies*, 2019, **4**, 1800420.
329. M. Miansari and J. R. Friend, *Advanced Functional Materials*, 2016, **26**, 7861-7872.
330. Z. Fan, H. Liu, M. Mayer and C. X. Deng, *Proceedings of the National Academy of Sciences*, 2012, **109**, 16486-16491.
331. N. Cermak, S. Olcum, F. F. Delgado, S. C. Wasserman, K. R. Payer, M. A. Murakami, S. M. Knudsen, R. J. Kimmerling, M. M. Stevens and Y. Kikuchi, *Nature biotechnology*, 2016, **34**, 1052-1059.
332. U. Demirci and G. Montesano, *Lab on a Chip*, 2007, **7**, 1139-1145.
333. C. Bouyer, P. Chen, S. Güven, T. T. Demirtaş, T. J. Nieland, F. Padilla and U. Demirci, *Advanced materials*, 2016, **28**, 161-167.
334. B. Kang, J. Shin, H.-J. Park, C. Rhyou, D. Kang, S.-J. Lee, Y.-s. Yoon, S.-W. Cho and H. Lee, *Nature communications*, 2018, **9**, 1-13.
335. T. D. Nguyen, V. T. Tran, Y. Q. Fu and H. Du, *Applied Physics Letters*, 2018, **112**, 213507.
336. C. Holtze, *Journal of Physics D: Applied Physics*, 2013, **46**, 114008.
337. FAO, *World fertilizer trends and outlook to 2022*, Rome, 2019.
338. G. T. Vladisavljević, N. Khalid, M. A. Neves, T. Kuroiwa, M. Nakajima, K. Uemura, S. Ichikawa and I. Kobayashi, *Advanced drug delivery reviews*, 2013, **65**, 1626-1663.
339. D. Conchouso, D. Castro, S. Khan and I. G. Foulds, *Lab on a Chip*, 2014, **14**, 3011-3020.
340. G. Tetradis-Meris, D. Rossetti, C. n. Pulido de Torres, R. Cao, G. Lian and R. Janes, *Industrial & engineering chemistry research*, 2009, **48**, 8881-8889.
341. T. Nisisako and T. Torii, *Lab on a Chip*, 2008, **8**, 287-293.
342. A. R. Abate and D. A. Weitz, *Lab on a Chip*, 2011, **11**, 1911-1915.
343. R. Schenk, V. Hessel, C. Hofmann, J. Kiss, H. Löwe and A. Ziogas, *Chemical Engineering Journal*, 2004, **101**, 421-429.
344. S. Togashi, T. Miyamoto, T. Sano and M. Suzuki, in *New Trends in Fluid Mechanics Research*, Springer, 2007, pp. 678-681.
345. B. Werner, V. Hessel and P. Löb, *Chemical Engineering & Technology: Industrial Chemistry-Plant Equipment-Process Engineering-Biotechnology*, 2005, **28**, 401-407.
346. I. Alfred and T. Pan, 1998.
347. E. Amstad, M. Chemama, M. Eggersdorfer, L. R. Arriaga, M. P. Brenner and D. A. Weitz, *Lab on a Chip*, 2016, **16**, 4163-4172.
348. A. Sealy, *Journal*, 2021.
349. M. Al-Rawashdeh, F. Yu, T. Nijhuis, E. Rebrov, V. Hessel and J. Schouten, *Chemical engineering journal*, 2012, **207**, 645-655.
350. M. Al-Rawashdeh, L. Fluitsma, T. Nijhuis, E. Rebrov, V. Hessel and J. Schouten, *Chemical Engineering Journal*, 2012, **181**, 549-556.
351. N. J. Straathof, Y. Su, V. Hessel and T. Noël, *Nature protocols*, 2016, **11**, 10-21.
352. F. Zhang, C. Cerato-Noyerie, P. Woehl and E. D. Lavric, *Chem. Eng. Trans*, 2011, **24**, 1369-1374.
353. K.-J. Wu, V. Nappo and S. Kuhn, *Industrial & Engineering Chemistry Research*, 2015, **54**, 7554-7564.
354. S. Gestermann, T. Bieringer, S. Buchholz and J. Heck, *Green Processing and Synthesis*, 2012, **1**, 535-537.
355. E. Novaresi, Ehrfeld Mikrotechnik BTS: a MIPROWA production reactor for Shaoxing Eastlake Biochemical - tks | publisher, event organiser, media agency. , https://www.teknoscienze.com/ehrfeld-mikrotechnik-bts-a-miprowa-production-reactor-for-shaoxing-eastlake-biochemical/).
356. S. K. Kurt, I. Vural Gürsel, V. Hessel, K. D. P. Nigam and N. Kockmann, *Chemical Engineering Journal*, 2016, **284**, 764-777.